Current state of the nanoscale delivery systems for temoporfin-based photodynamic therapy: Advanced delivery strategies

Ilya Yakavets, Marie Millard, Vladimir Zorin, Henri-Pierre Lassalle, Lina Bezdetnaya

Current state of the nanoscale delivery systems for temoporfin-based photodynamic therapy: advanced delivery strategies

Ilya Yakavets[a,b,c], Marie Millard[a,b], Vladimir Zorin[c,d], Henri-Pierre Lassalle[a,b], Lina Bezdetnaya[a,b,*]

[a] Centre de Recherche en Automatique de Nancy, Centre National de la Recherche Scientifique UMR 7039, Université de Lorraine, Campus Sciences, Boulevard des Aiguillette, 54506 Vandoeuvre-lès-Nancy, France;

ilya.yakavets@nancy.unicancer.fr (I.Y.); marie.millard@nancy.unicancer.fr (M.M.) ; h.lassalle@nancy.unicancer.fr (HP.L.)

[b] Research Department, Institut de Cancérologie de Lorraine, 6 avenue de Bourgogne, 54519 Vandoeuvre-lès-Nancy, France

[c] Laboratory of Biophysics and Biotechnology, Belarusian State University, 4 Nezavisimosti Avenue, 220030 Minsk, Belarus;

zorin@bsu.by (V.Z.)

[d] International Sakharov Environmental Institute, Belarusian State University, Dauhabrodskaja 23, 220030 Minsk, Belarus

*** Correspondence to:** Lina Bezdetnaya. l.bolotine@nancy.unicancer.fr; Tel.: +33-(0)3-08-59-83-53

Address : Institut de Cancerologie de Lorraine, 6 Avenue de Bourgogne – CS 30519, 54519 Vandoeuvre-les- Nancy, Cedex, France.

Author contributions: IY, MM - Writing – Original Draft; HPL, VZ, LB - Writing – Review & Editing; VZ, LB – Supervision.

Abstract

Enthusiasm for photodynamic therapy (PDT) as a promising technique to eradicate various cancers has increased exponentially in recent decades. The majority of clinically approved photosensitizers are hydrophobic in nature, thus, the effective delivery of photosensitizers at the targeted site is the main hurdle associated with PDT. Temoporfin (mTHPC, medicinal product name: Foscan®), is one of the most potent clinically approved photosensitizers, is not an exception. Successful temoporfin-PDT requires nanoscale delivery systems for selective delivery of photosensitizer. Over the last 25 years, the number of papers on nanoplatforms developed for mTHPC delivery such as conjugates, host-guest inclusion complexes, lipid-and polymer-based nanoparticles and carbon nanotubes is burgeoning. However, none of them appeared to be "ultimate". The present review offers the description of different challenges and achievements in nanoparticle-based mTHPC delivery focusing on the synergetic combination of various nano-platforms to improve temoporfin delivery at all stages of biodistribution. Furthermore, the association of different nanoparticles in one nanoplatform might be considered as an advanced strategy allowing the combination of several treatment modalities.

Keywords: drug delivery; hybrid nanodelivery systems; nanoparticles; photodynamic therapy; temoporfin

Graphical abstract

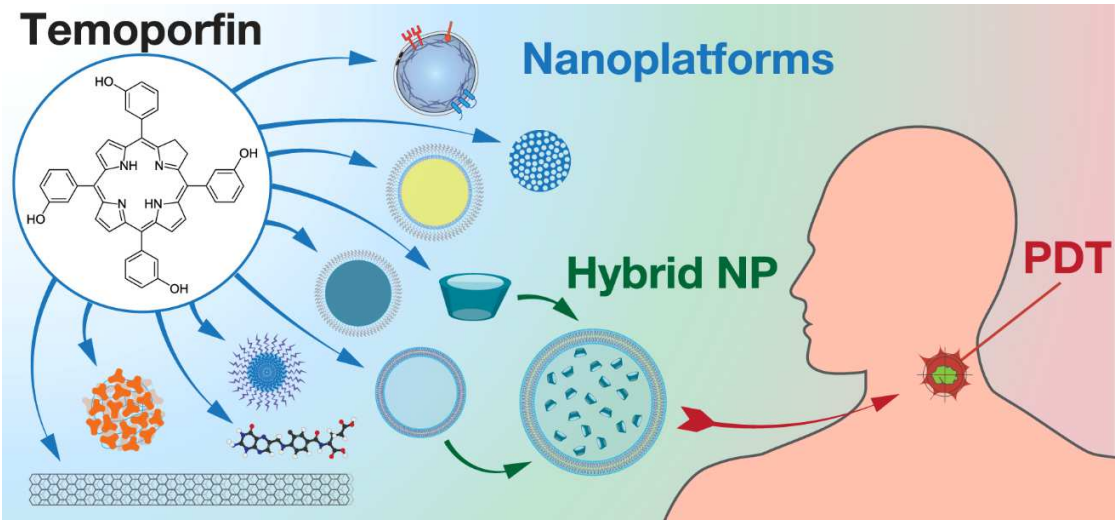

OUTLINE

1. Introduction

Photodynamic therapy (PDT) is a promising minimally invasive treatment, commonly used in medical disciplines, such as dermatology, oncology, gynecology and urology [1]. PDT has been approved for palliative treatment of head and neck tumors, basal-cell carcinoma, biliary tract cancer, lung cancer, T-cell lymphoma and age-related macular degeneration [2]. Currently, clinical trials with PDT are proposed for a wide range of solid tumors, including the brain, breast, lung, pancreas, and prostate. Good therapeutic results and the possibility of combining PDT with other therapeutic modalities in cancerology defines its attractivity [3].

Phototherapeutics termed photosensitizers (PSs), exhibit the properties such as (i) photo-reactivity; (ii) not-toxicity in the absence of light; (iii) specific accumulation in tumor tissues; (iv) selectivity conferred by a light beam; (v) photocytotoxic activity against targeted cells. Upon light excitation, these molecules generate cytotoxic reactive oxygen species (ROS), inducing cell death and tissue destruction. The efficiency of ROS generation is mainly determined by photophysical properties of PS and penetration ability of excitation light across the tissue. Thus, to be effective PS should possess a high quantum yield of ROS generation and strong absorption in the red and/or infra-red spectral regions [4]. The effectiveness of PDT is also determined by PS pharmacodynamics and biodistribution. Inasmuch as the main intermediator, singlet oxygen, a highly reactive species with a short half-life in biological systems (less than 40 ns) [5], directly affects only molecules and structures that are proximal to the area of its production [6]. Therefore, precise delivery and accurate localization of PS at target sites are required for effective PDT.

Over the last decades, it has been demonstrated that the combination of photosensitizers with nanomaterial platforms enable precise delivery of PS to the target tissues improving the PDT effectiveness. Nanoparticles (NPs) can have numerous advantages as a PS delivery system, such as

(i) protection of the PS against enzymatic degradation; (ii) the control release of PS allowing a constant and uniform concentration into the target cells; (iii) the ability to penetrate target tissues due to their submicron size; (iv) biocompatibility and resorbability through natural pathways and (v) photostability. Moreover, since the most effective PSs tend to be insoluble hydrophobic molecules with a high propensity to aggregate, their encapsulation into nanocarriers could improve their pharmacokinetic properties. Additionally, nanotechnology-based drug delivery systems provide the opportunity for active targeting and for application of multimodal combined therapies.

The present review focuses on the nanoparticle-based delivery systems of potent clinically approved PS temoporfin. Among other second-generation photosensitizers, temoporfin possesses unique biopharmaceutical properties defining its high PDT potency. Since the last decade, about 10 reports per year on temoporfin nanoparticles have been published and this number is constantly increasing. However, a state-of-the-art review of *in vitro* and *in vivo* aspects of nanovehicle-based temoporfin delivery, along with a critical discussion of nanoformulations design parameters, perspectives, and challenges regarding *in vivo* drug distribution is not currently available. Therefore, we have attempted to provide the comprehensive review, aiming to guide future research in photonanomedicine using temoporfin. The successive sections summarize the investigations on the strategies aiming the development of nanotechnology-based temoporfin delivery systems in PDT.

2. **Temoporfin**

5,10,15,20-Tetrakis(3-hydroxyphenyl)chlorin (mTHPC, temoporfin), the standard chlorin-based photosensitizer (PS) since its discovery in the 1980s, is one of the most potent second generation photosensitizers currently available in clinical PDT. In 2011, Senge and Brandt comprehensively reviewed the general aspects of mTHPC application in clinics [7]. Temoporfin was already clinically approved in European Union in 2001 for the treatment of head and neck squamous

cell carcinoma using an ethanol anhydrous/propylene glycol-based commercial formulation (Foscan®; biolitec pharma Ltd., Jena, Germany) [8,9]. In clinical PDT mTHPC is applied at both a very low drug dose (0.15 mg kg^{-1}) and light intensity (order of 10 J cm^{-2}) resulting in a total PDT dose (light dose × PS dose) more than 100 times lower compared with other clinically approved PSs, such as haematoporphyrin derivatives [10,11] and Photofrin [12].

Photophysical properties of mTHPC were intensively investigated [13,14] and it appears that they solely cannot account for the high mTHPC-PDT efficacy. Other PS as bacteriochlorin-type TOOKAD® or tin ethyl etiopurpurin (Purlytin™) are also characterized by a high extinction coefficient (90,000 $M^{-1}cm^{-1}$ at 763 nm) [15] or high quantum yield of singlet oxygen $\Phi_\Delta = 0.7$ [16]. Therefore, the moderate values of both extinction coefficient (30,000 $M^{-1}cm^{-1}$) and quantum yield of singlet oxygen ($\Phi_\Delta = 0.43$), as well as the long wavelength of absorbance at 652 nm, could not be the only responsible for high PDT efficiency (Figure 1). Thus, it was supposed that the benefits of mTHPC application mainly rely on the capacity of mTHPC to sequester tightly in cells along with its photophysical properties [17].

Nevertheless, mTHPC-PDT is still not optimal, leaving a much room for improvement. The essential challenge of mTHPC delivery is its poor water-solubility. As a rule, mTHPC is intravenously introduced to the patients as a solution for i.v. injection (Foscan®) containing 1 mg of temoporfin in a 1 ml of a mixture of ethanol anhydrous and propylene glycol [9] in order to palliate its high hydrophobic nature. mTHPC molecules possess octanol-water partition coefficients (logP) greater than 3 [18], thus hydrophobic nature defines its pharmacokinetics and biodistribution behavior. Administration of mTHPC as Foscan® formulation prevents the effective formation of non-photoactive aggregates in blood flow after its injection resulting in distorting the pharmacokinetics and reducing drug bioavailability. Foscan® formulation should be injected slowly

to avoid drug precipitation at the injection site, however, its administration is accompanied by pain [19].

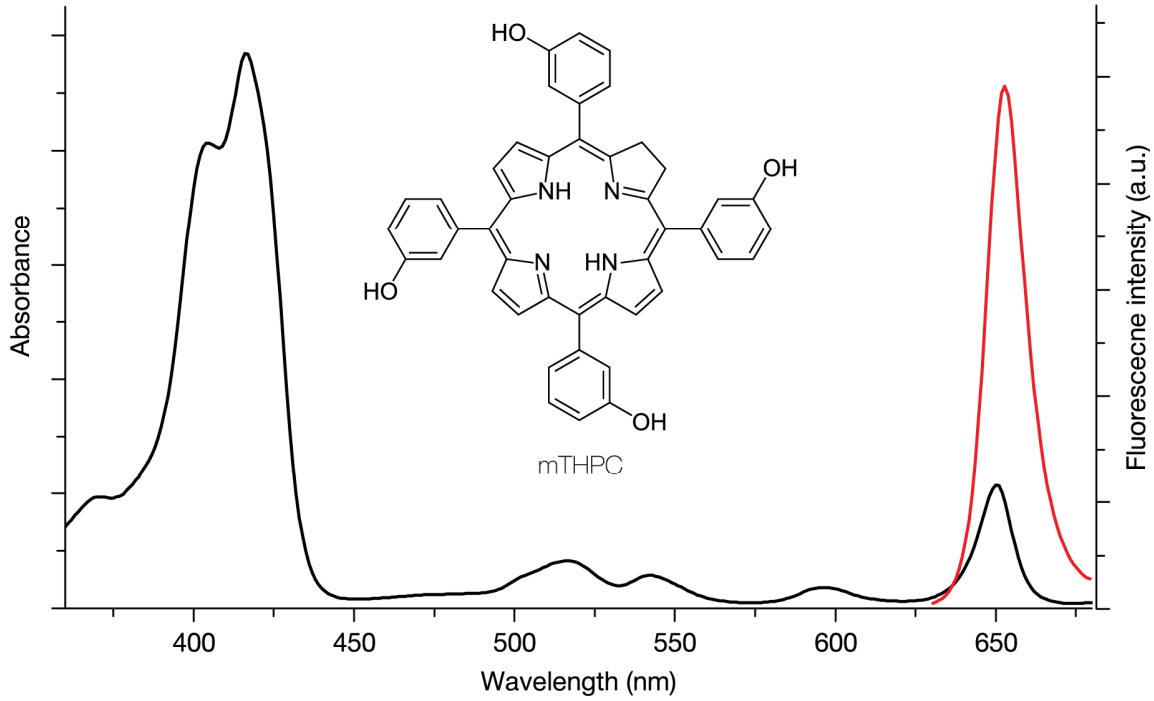

Figure 1. Absorbance (black) and fluorescence (red) spectra of mTHPC in methanol. Adapted and reprinted with permission from ref [20].

More importantly is that mTHPC molecule is highly lipophilic. Lipophilic nature determines its high affinity for lipid microenvironment as lipoproteins or cellular membranes [21–23]. Thus, complete or partial disaggregation could happen in the circulation upon interaction with blood components, mostly cells and serum lipoproteins [21]. Nevertheless, high mTHPC lipophilicity hampers its diffusion through aqueous surrounding making the redistribution process of PS between binding sites extremely slow [24]. Hereby, a considerable amount of PS moves from aggregates to blood components and further slowly redistributes to target cells. This is why the drug-light interval

(DLI) for Foscan® is up to several days [7,25], while Verteporfin-PDT may be performed at a dozen minutes after the PS administration [25]. Even when mTHPC reaches the tumor tissue, high lipophilicity leads to the limited PS penetration into the tumor stroma, as was demonstrated on multicellular tumor spheroids and *in vivo* pre-clinical models [17,26,27]. This could be a reason for tumor relapse sometimes observed after PDT. Finally, mTHPC noticeably accumulates in the skin that together with the extremely slow release of mTHPC from the cells [17] results in a prolong post-treatment skin photosensitivity [28]. Eye and skin preservation for 6 weeks after mTHPC injection should be also considered in clinical settings. Most common side effects of Foscan®-based PDT are headache, hemorrhage, dysphagia and edema [29]. Overcoming the mentioned challenges in PS biodistribution could be possible by application of nanomedicine facilities. The use of nanocarriers based on polymers, lipids or non-organic materials provides the opportunity to facilitate administration of hydrophobic drugs as mTHPC and to tune its pharmacokinetics.

3. **Nanodelivery systems for temoporfin**

The attempts of NP-based mTHPC delivery have been made since 1995 [30,31]. Currently, numerous nano-platforms based on a variety of organic and inorganic nanomaterials have been studied for efficient and targeted mTHPC delivery (Figure 2). Various strategies of passive and active transport of mTHPC were conducted. Hereafter we review in details all nanoscale-based mTHPC formulations in terms of structural, photophysical and biopharmaceutical properties. The nanoparticles will be present in function of their size and complexity for easy following this review. We will describe the conjugates, inclusion complexes, polymeric and lipid-based NPs, ending up with carbon-based nanostructures. In conclusion, hybrid delivery systems for mTHPC will be reviewed.

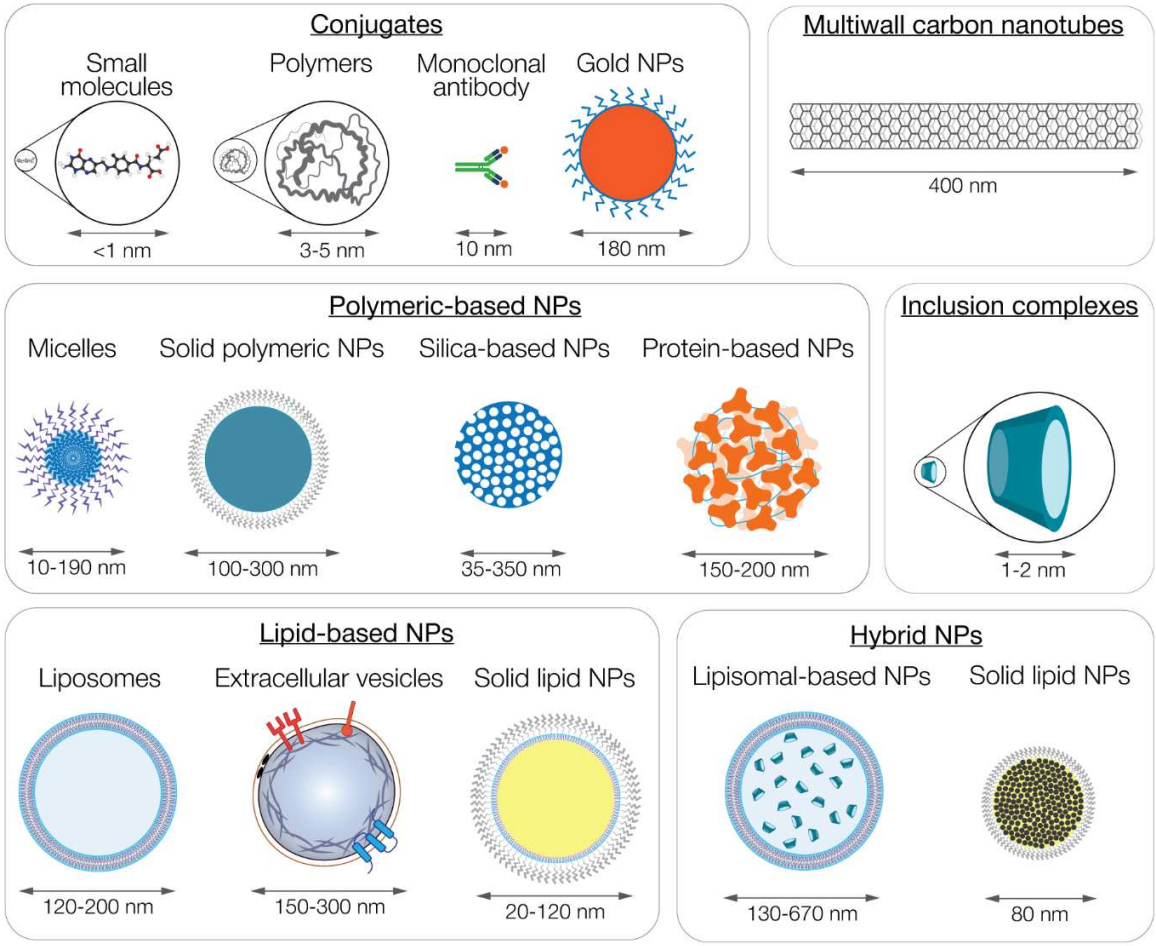

Figure 2. Nanoplatforms already applied for mTHPC delivery

The main observations on temoporfin nanocarriers, which achieved *in vitro* and *in vivo* evaluation in pre-clinical models, are presented in the Table 1.

Table 1. Temoporfin-loaded nanoplatforms in biological studies

NP	Targets	Observations	Ref.
Conjugates			
PEG	Nude mouse bearing xenografts LS174T, chinese hamster with induced early squamous cell carcinoma in the cheekpouch mucosa	Compared with free mTHPC: longer plasma half-time and lower liver uptake; lower penetration depth in the tumor tissue *in vivo*; higher the maximal tumor-to-muscle ratio *in vivo*; no selectivity in early squamous carcinoma cells *in vivo* (hamster mucosa); no significant difference after PDT.	[30, 31]
	Nude mice bearing xenografts Colo26	Compared with free mTHPC: increased plasma half-time; lower tumor necrosis depth *in vivo*; no significant muscle damages; PEG chain length had relatively little effect on the patterns of mTHPC bioactivity.	[32, 33]
	Nude mouse bearing human squamous cell carcinoma and adenocarcinoma xenografts; minipig	Larger tumor necrosis in squamous cell carcinoma, but not in adenocarcinoma xenografts in mice *in vivo* compared with free mTHPC. No visible normal tissue alterations after mTHPC-PEG administration in minipigs *in vivo*.	[34]
	Female RAG-2-mice bearing xenografts XF 354	No significant therapeutic effect observed *in vivo*.	[35]
Glycose	HT29 monolayer cells	The asymmetric TPC(m-O-GluOH)$_3$ exhibited higher phototoxicity *in vitro* compared to free mTHPC. An active receptor-mediated endocytosis mechanism of conjugates' internalization. Intracellular localization in mitochondria.	[18]
Folic acid	HT29 and KB monolayer cells; nude mouse bearing xenografts HT29 and KB	Active targeted accumulation in KB tumors *in vivo* compared with free mTHPC	[36]
Monoclonal antibodies	UM-SCC-22A, UM-SCC-22A, UM-SCC-22B, HNX-OE monolayer cells; nude mouse bearing xenografts HNX-OE	Stable in serum. Low dark toxicity along with decreased intracellular accumulation and PDT efficiency *in vitro.* Selective targeting of the sensitizer to the tumor *in vivo*.	[37, 38]
Non-steroidal anti-inflammatory drugs	SKGT-4, OE33 monolayer cells	All conjugates successfully entered the cells and whilst no cytotoxicity *in vitro* was observed.	[39]
Gold nanoparticles (180 nm)	SH-SY5Y monolayer cells	Internalization in cells *in vitro* was confirmed. Lower dark toxicity and increased photocytotoxicity *in vitro* compared to free mTHPC.	[40]
Inclusion complexes			
β-cyclodextrin derivatives	Monolayer HT29 cells; multicellular HT29 spheroids; nude mouse bearing xenografts HT29	Compared with free mTHPC: enhanced uptake and phototoxicity in cells *in vitro*; increased accumulation and deeper penetration in spheroids *in vitro*; higher tumor-to-skin and tumor-to-muscle ratios *in vivo.*	[41, 42]
Micelles			
mPEGG750 polymers (10 nm)	14C monolayer cells	The uptake and phototoxicity of mTHPC in cells *in vitro* were observed only after degradation of micelles	[43]

pH-responsive PEOz-*b*-PLA (180-190 nm)	HT29 monolayer cells	mTHPC oil/water nanoemulsion displays lower cellular uptake *in vitro* compared with Foscan®	[44]
pH-responsive PEOz-*b*-PLA (77 nm)	HT29 monolayer cells; nude mouse bearing xenografts HT29	Low cellular uptake and phototoxicity *in vitro* compared to free mTHPC. Similar to free mTHPC antitumor effects *in vivo* significantly reduced skin photosensitivity *in vivo*.	[45]
pH-responsive PEGMA-co-DPA (132-156 nm)	HT29 monolayer cells	Lower cellular uptake *in vitro* with preferable localization in lysosomes. Comparable with free mTHPC phototoxicity *in vitro*	[46]
Chitosan oligosaccharide nanoparticles (130-145 nm)	U87MG monolayer cells; multicellular U87MG spheroids; nude mouse bearing xenografts U87MG	VES-g-CSO/TPGS/RGDfK nanoparticles exhibit higher cellular uptake and photocytotoxicity *in vitro*. Deeper penetration and better photodynamic effect in spheroids *in vitro*. Enhanced antitumor efficiency *in vivo*.	[47]
Lipid-DNA polymer (8-10 nm)	A431, HT29, L929, J744A1.1, CAL27 monolayer cells	Compared with free mTHPC, lower dark cytotoxicity and higher PDT efficiency in cells *in vitro*	[48]
Ben-PCL-mPEG (16-57 nm)	RAW264.7, C166 C166 monolayer cells; nude mouse; LDLR−/−ApoB100/100 mouse	Selective photocytotoxicity in macrophages compared with endothelial cells *in vitro*. Similar to free mTHPC pharmacokinetics in plasma *in vivo*	[49]
Solid polymeric nanoparticles			
Ultrafine hydrogel nanoparticles (2-3 nm)	C6 monolayer cells	PDT efficacy *in vitro* similar to free mTHPC PDT	[50]
PLGA nanoparticles (283 nm)	HT29 monolayer cells	Similar to free mTHPC both accumulation in cells and penetration into spheroids *in vitro*. Reduction of dark cytotoxicity. Time- and concentration-dependent decrease in cell proliferation and viability *in vitro* after PDT similar to free mTHPC.	[51]
PLGA-PEG nanoparticles (145-180 nm)	A549, MCF10A U937; nude mouse bearing xenografts HCT-116-luc	PEGylation reduced mTHPC uptake in cells *in vitro*. Reduced dark cytotoxicity along with equal PDT efficacy *in vitro* as for free mTHPC. The therapeutically favorable tissue distribution *in vivo*.	[52]
PLGA-PEG nanoparticles (97 nm)	J774.A1, HT29 monolayer cells; male CD-11 Crl:CD1(ICR) mouse	Reduced dark cytotoxicity along with equal PDT efficacy *in vitro* compared with free mTHPC. Improved *in vivo* distribution after injection.	[53]
Silica-based nanoparticles			
Organically modified silica nanoparticles (33 nm)	KYSE 510 monolayer cells	Reduced intracellular uptake, however similar to free mTHPC phototoxicity *in vitro*.	[54]
Calcium phosphate nanoparticles (170-205 nm)	CAL-27 monolayer cells; nude mouse bearing xenografts CAL-27	Calcium phosphate nanoparticles/temoporfin/RGDfK peptide/DY682-NHS platform. RGDfk targeting decreased intratumoral accumulation and enhanced uptake in the lungs *in vivo*. Therapeutic success was achieved with 3 of 4 mice *in vivo*.	[55]

Silica-based nanoparticles (166-350 nm)	4T1, MDA-MB-231 monolayer cells; nude mouse bearing xenografts MDA-MB-231	Comparable with free mTHPC intracellular uptake *in vitro*. Higher antitumor PDT effect *in vivo* compared to Foscan®. Penetration through the blood-brain barrier was confirmed.	[56]
Protein-based nanoparticles			
HSA nanoparticles (150-200 nm)	Jurkat monolayer cells	The singlet oxygen generation inside Jurkat cells *in vitro* was confirmed. Similar cellular uptake and phototoxicity *in vitro* as free mTHPC. Preferable intracellular localization in lysosomes.	[57, 58]
Liposomes			
Foslip® (135 nm)	Fertilized chicken egg	Significant vascular damage in chick chorioallantoic membrane *in ovo* at high drug dose (1 mg/kg b.w.) and at a minimally effective light dose > 25 J/cm^2.	[59]
	Nude mouse with induced skin carcinoma	Significant selectivity between the lesion and normal surrounding skin at 4 h.	[60]
	Nude mouse bearing xenografts HT29	High selectivity *in vivo*: the average tumor-to-muscle and the tumor-to-skin selectivity were 6.6 and 2, respectively. Rapid biodistribution and clearance from the bloodstream.	[61]
	GBC, BDC monolayer cells	Lower accumulation and dark toxicity in cells *in vitro* compared to Foscan®. Almost identical behavior of both formulations in the presence of serum.	[24]
	Nude mouse bearing xenografts EMT6	Slow mTHPC release from liposomes and inhomogeneous distribution in the tumor *in vivo* after intratumoral administration. Optimal, albeit partial, cure rates at 24 h post-administration.	[62]
	HeLa monolayer cells	Similar to Foscan®uptake in tumor cells *in vitro*. The decrease of mTHPC fluorescence life-times during incubation.	[63]
	Female Foxn1$^{nu/nu}$ mouse bearing xenografts EMT6	Tumor-to-muscle ratio *in vivo* was 3.6 from 6 to 15 h DLI. Illumination intervals at 6 and 15 h were the most effective in terms of growth delay.	[64]
	Nude female SKH-1 mouse	Significant acceleration of wound healing after PDT *in vivo.*	[65]
	PC-3 monolayer cells	Foslip®-based PDT resulted in severe damage of both RNA and DNA *in vitro.*	[66]
	Female Fisher-344 rat bearing xenografts R3230AC	Higher bioavailability *in vivo* than Foscan®.	[67]
	Male Wistar rats with induced carcinoma of oral epithelium	Comparable to Foscan® fluorescence in the subepithelial stroma *in vivo*. Higher fluorescence in the tumor *in vivo* at 2, 4, and 8 hours compared to Foscan®.	[68]
	Free and EMT6 xenografted fertilised chicken eggs	Quick destruction of liposomes in blood in chick chorioallantoic membrane *in ovo*. The destruction and occlusion of the smaller vessel at 1 h DLI and total occlusion of the treated area at 3 h DLI after PDT *in ovo*. Tumor necrosis was 30 % at 15 min as well as at 1 h DLI.	[69]
	Nude mouse bearing xenografts HT29	Quick drug efflux from Foslip® in plasma *in vivo*. High elimination rate from the skin *in vivo*. Release from vasculature to tumor stroma at 15 h. Tumor growth delay was 44.4 days at 24h DLI.	[70]
	Nude mouse bearing xenografts CAL-27	PDT-induced apoptosis and tumor vascularization damage *in vivo* at 2 days after treatment. Decrease of tumor volume at 20 days after PDT.	[71]
	Female C57BL/6 mouse with induced acute colitis	Reduced intestinal tumor growth *in vivo*. Prevention of a dysbiotic microbiota in colitis-associated cancer *in vivo* model.	[72]

	HeLa monolayer cells; multicellular HeLa spheroids	Higher uptake and lower dark cytotoxicity in monolayer cells *in vitro* compared to free mTHPC. Less homogeneous distribution in spheroids *in vitro* than free mTHPC. Slightly better PDT efficiency in monolayer cells and in spheroids *in vitro* than free mTHPC.	[73]
	Nude mouse bearing xenografts CAL-33	The increased tumor-to-skin ratio *in vivo* compared to free mTHPC. Enhanced accumulation of mTHPC in all tissues. The better therapeutic antitumor effect *in vivo* than free mTHPC.	[74]
	143B, K7M2L2 monolayer cells; female SCID mouse bearing xenografts 143B; female BALB/c mouse bearing xenografts K7M2L2	No significant difference, lower dark cytotoxicity and higher PDT efficiency in cells *in vitro* compared to Foscan®. Enhanced uptake in tumor and slightly higher antitumor efficiency *in vivo* compared to Foscan®. Similar to Foscan® effect on pulmonary metastases and tumor perfusion *in vivo*.	[75]
	Multicellular HT29 spheroids	Limited penetration of mTHPC in spheroids *in vitro*.	[76]
	HT29 monolayer cells; multicellular HT29 spheroids	Lower accumulation in cells *in vitro* compared to free mTHPC. Low penetration ability of mTHPC in spheroids *in vitro*.	[77]
Fospeg® (125 nm)	Cats bearing cutaneous squamous cell carcinoma xenografts	Several times higher tumor accumulation, therapeutic ratio, plasma concentration and bioavailability in cats *in vivo* compared to Foscan®	[78]
	Fertilized chicken egg	Higher vascular damage in chick chorioallantoic membrane *in ovo* compared to Foslip®	[59]
	A431 monolayer cells	Similar uptake and retention in cells *in vitro*. Reduced dark and photoinduced cytotoxicity effects *in vitro*.	[79]
	A549, CCD-34Lu monolayer cells	Lower accumulation, dark cytotoxicity and photocytotoxicity in cells *in vitro* compared to free mTHPC.	[80]
	Female Fisher-344 rat bearing xenografts R3230AC	Higher bioavailability *in vivo* than Foscan®. The highest tumor fluorescence *in vivo* at the earlier time points compared to Foslip® and Foscan®.	[67]
	Female Wistar rat bearing xenografts MC28	Decreased plasma clearance and lower skin photosensitivity *in vivo* compared to Foscan®. Increased accumulation in the tumor *in vivo* and the tumor-to-skin ratio was 6. A greater percentage of tumor necrosis at low dose PDT.	[81]
	LNCaP monolayer cells	Enhanced intracellular uptake and photodynamic activity in cells *in vitro*.	[82]
	Male Wistar rats with induced carcinoma of oral epithelium	Higher fluorescence in normal and tumor tissue *in vivo* compared to both Foscan® and Foslip®.	[68]
	Free and EMT6 xenografted fertilised chicken eggs	Significantly higher stability, slower drug release, better tumoricidal effect and lower damage to the normal vasculature in chick chorioallantoic membrane *in ovo* at already 1 h DLI as compared to Foslip®.	[69]
	Nude mouse bearing xenografts HT29	Higher levels for the first 6 hours in plasma *in vivo* compared to Foslip®. Slow release form vasculature *in vivo*. Higher *in vivo* PDT efficiency at shorter DLI compared to Foslip®.	[70]
	Nude mouse bearing xenografts HT29	The rapid uptake of mTHPC in the liver *in vivo* followed by a fast clearance. Tumor-to-skin ratio was 3.8 at 2 h.	[83]
	C666-1, HK1, CNE2 monolayer cells	No P-gp-mediated efflux in cells *in vitro*. Induction of over-expression of MDR1 gene transcript and P-gp proteins after PDT.	[84]
	HeLa monolayer cells; multicellular HeLa spheroids	No significant differences in penetration and PDT efficiency in spheroids *in vitro* compared to Foslip®	[73]
DMPC/Gemini	COLO206, LN229, U118, A172, DBTRG, C6 monolayer	Cationic gemini surfactant increased mTHPC cellular uptake	[85–

liposomes	cells	and resulted in a high grade of photocytotoxic effect *in vitro*.	88]
Invasomes (105-170 nm)	Nude mouse bearing xenografts HT29	Treatment with mTHPC-loaded invasomes with 1 % terpene mixture resulted in a slower increase in tumor size *in vivo*	[89]
	Human female abdominal skin	The increase of mTHPC amount in deep stratum corneum and deeper skin layers *in vitro* compared to free mTHPC	[90]
Flexosomes	Human abdominal skin	Cationic flexosomes delivered the highest mTHPC amount to stratum corneum and deeper skin layers compared to anionic and neutral ones.	[91]
Extracellular vesicles (180 nm)	CT26 monolayer cells; multicellular CT26 spheroids	Enhanced uptake in cancer cells and equivalent penetration potential in spheroids *in vitro* compared to free mTHPC and Foslip®.	[92]
	HT29 monolayer cells; multicellular HT29 spheroids	Increased stability in plasma compared Foslip®. Enhanced accumulation and photocytotoxicity in cells *in vitro*. Deeper penetration and higher PDT efficiency in spheroids *in vitro*.	[77]
Solid lipid nanoparticles			
M-Lipidots (18-80 nm)	MCF-7 monolayer cells	Mild dark and photoinduced cytotoxicity *in vitro* for naked lipid nanodroplets.	[93]
M-Lipidots (50-120 nm)	CAL-33 monolayer cells; multicellular CAL-33 spheroids; nude mouse bearing xenografts CAL-33	Lower uptake in cells and deeper penetration in spheroids *in vitro* compared with free mTHPC. Reduced dark cytotoxicity in cells and spheroids *in vitro.* Increased mTHPC uptake in all tissues *in vivo* compared to Foscan®. Comparable tumor volume reduction with Foscan®.	[74, 94]
Thermoresponsive solid lipid nanoparticles (50 nm)	4T1, MDA-MB-231 monolayer cells; nude mouse bearing xenografts MDA-MB-231	Compared with free mTHPC: faster accumulation and higher phototoxicity *in vitro*; improved anticancer efficacy *in vivo.*	[95]
Non-organic nanoparticles			
Multi-walled carbon nanotubes (400 nm)	SKOV3 monolayer cells	Carbon nanotubes internalized in the cells *in vitro* with subsequent mTHPC release to the cellular compartments. Synergic impact of the combined photothermal/photodynamic therapy *in vitro.*	[96]
Hybrid nanoparticles			
Theranosomes with magnetic nanoparticles (670 nm)	SKOV-3, PC3, TC-1 monolayer cells; nude mouse bearing xenografts TC-1	Enhanced uptake by cancer cells and cellular death due to the magnetic targeting *in vitro.* The increased antitumor effect *in vivo*.	[97, 98]
Ultramagnetic Photosensitive Liposomes (150 nm)	SKOV-3 monolayer cells; nude mouse bearing xenografts A431	Synergetic antitumoral PDT efficacy *in vitro*. Complete eradication of the tumor *in vivo* by combined magnetic/photodynamic therapy.	[99]
Upconversion nanoparticles in solid lipid nanospheres (80 nm)	ALTS1C1, bEnd.3 monolayer cells; male C57BL/6J mice bearing orthotopic ALTS1C1 tumor	Upconversion nanoparticles/IR-780/mTHPC/C-PEG-maleimide nanoparticles. Higher accumulation in cells *in vitro* compared to free mTHPC. Synergetic antitumoral efficacy *in vitro* after photothermal/photodynamic therapy. Overcoming a blood-brain barrier and enhanced mTHPC accumulation in brain tumor *in vivo*. Increased median survival after combined therapy *in vivo*.	[100]

Drug-in-cyclodextrin-in-liposome (126-143 nm)	HT29 monolayer cells; multicellular HT29 spheroids	Similar to Foslip® accumulation in cells and spheroids *in vitro*. Complete penetration and homogeneous distribution of mTHPC across the spheroid *in vitro*.	[76]

3.1. Conjugates

Chemical conjugation of therapeutics with active molecules is one of the oldest strategies of biopharmaceutical improvement. This strategy was applied to introduce the third generation photosensitizers and was comprehensively reviewed by Senge [28]. There are many types of common biomolecules which are suggested to be conjugated with mTHPC to improve its solubility, *i.e.* polymers [32,33], to increase drug selectivity against tumor, *i.e.* glucose [18,101], folic acid (FA) [36], monoclonal antibodies [37,38] or to overcome the post-treatment side effects using anti-inflammatory agents *i.e.* ibuprofen [39] (Figure 3). It should be noted, that covalent linkage may be subjected to damage in biological media and may also affect photophysical properties of dyes.

The simplest way to solubilize drug is to prevent the interaction between its molecules. Poly(ethylene)glycol (PEG) is considered as a common solubilizing molecule, which could be covalently bound to mTHPC, according to the patent of Sinn & co-workers in 1991 [102]. The hydrodynamic diameter of PEG depends on the polymerization degree (i.e. 3 and 5 nm for PEG-2000 and PEG-5000, respectively) [103]. Following the optimization of conjugates, the degree of PEG polymerization varied and mTHPC-PEG-2000 was pre-selected for further *in vitro* studies due to its stability in biological media and a lowest dark toxicity in Colo26 colorectal tumor cells [33]. Obviously, PEG conjugates prevent mTHPC aggregation as well as the PS interactions with lipoproteins. Moreover, PEG molecules commonly have a limited intracellular accumulation that theoretically could reduce PDT efficiency. Practically, solubilization of mTHPC due to conjugation with PEG prolongs 2 times its half-time in murine plasma [104] and significantly improves

selectivity, demonstrating a better accumulation in human LS174T colon carcinoma xenografts (tumor-to-muscle ratio up to 20) and a lower level in liver compared with free mTHPC [30]. Nevertheless, the photodynamic efficiency of mTHPC-PEG compounds did not exceed that of free mTHPC in xenografts [30–32,34,35].

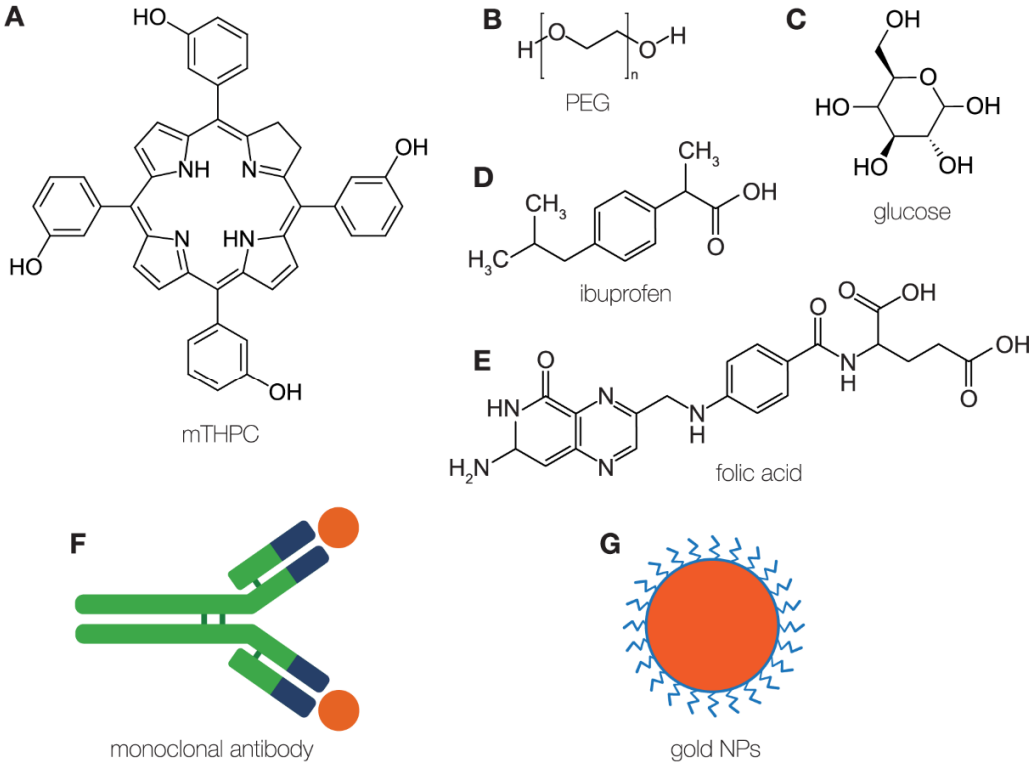

Figure 3. Active molecules, which could covalently bound to (A) mTHPC: (B) poly(ethylene-glycol) (PEG), (C) glucose, (D) ibuprofen, (E) folic acid, (F) monoclonal antibody, (G) gold NPs.

Another strategy is to use small active molecules as solubilizers for mTHPC. For example, glucose [18] and FA [36] (the size is <1 nm [105]) were conjugated with mTHPC and modulated its water solubility by creating a balance between hydrophilicity and hydrophobicity. Additionally, in

the case of glucose, it has been hypothesized that targeting of glucose metabolism may provide a selective targeting of cancer due to the Warburg effect [106]. However, *in vitro* studies performed using glucosylated mTHPC demonstrated less intracellular uptake in human colorectal adenocarcinoma (HT29) monolayer cells than that of the free drug [18]. Nevertheless, photodynamic efficiency was increased in the case of (TPC(*m*-*O*-Glu)$_3$) compared with symmetrical (TPC(*m*-*O*-Glu)$_4$) and free mTHPC. At the same time, water-soluble vitamin B9 or FA could be used as targeting agents for cancers that overexpress folate receptor (FR-α) on their cellular membrane, like ovarian, breast and lung cancers [107]. In 2008, Gravier et al. tested FA-conjugated mTHPC in a mouse xenograft model *in vivo* using KB cells rich in FR-α and HT29 cells as a negative control [36]. This study indeed demonstrated that FA-mTHPC conjugates were strongly accumulated in the KB tumors with a tumor/normal tissue ratio more than 5.0, compared with that of 2.1 for free mTHPC; equal accumulation was noted for both formulations in HT29 tumors.

The selectivity of the drug against a specific cancer type could be achieved using tumor-selective monoclonal antibodies. With this aim, Vrouenraets and co-workers conjugated mTHPC with neck squamous cell carcinoma-selective chimeric monoclonal antibody (cMAb) U36 [37,38]. The size of cMAb is about 10 nm, as was estimated for IgG [103]. Despite the optimistic *in vitro* results on serum stability and immunoreactivity, mTHPC loading ratio was only several molecules per cMAb that was not enough for efficient PDT treatment of U36 monolayer cells *in vitro*. The experiments *in vivo* in tumor-bearing mice demonstrated that the tumor/skin ratio was 3.5 times higher compared with mTHPC, nevertheless it was concluded that successful PDT application of mTHPC-MAb conjugates requires a high level of total conjugate binding and is possible only for internalized MAbs.

To go further in order to improve PDT therapeutic efficacy, the combined therapy using non-steroidal anti-inflammatory drugs was proposed. Rogers and co-workers theorized that a conjugate

will undergo biological cleavage to deliver the PS and anti-inflammatory drug at the tumor site [39]. With this aim, they successfully synthesized the library of "iPorphyrins" composed of mTHPC conjugates with non-steroidal anti-inflammatory drugs to specifically target the tumor microenvironment. However, the covalent linking of mTHPC to non-steroidal anti-inflammatory drugs significantly reduced the efficiency of singlet oxygen production. Therefore, it is not surprising that the phototoxic effect was not observed in the esophageal carcinoma OE33 and SKGT-4 cells despite the successful intracellular accumulation of conjugates. It is one of the examples of how covalent binding of mTHPC with biomolecules influences photophysical properties of PS thus complicating the prediction of photodynamic response of such compounds using standard uptake studies *in vitro*.

Finally, mTHPC could be conjugated with nanoplatforms such as gold nanopartcles (AuNPs). AuNPs are non-toxic, biocompatible and provide a relatively long circulation time of drug bound to their surface [108]. Haimov with co-workers synthesized 180-nm mTHPC-AuNPs allowing to passively target the hyper-permeable tumors taking the benefits of enhanced permeability and retention (EPR) effect [40]. This also offered an opportunity to use mTHPC-AuNPs as contrast agents for computed tomography imaging *in vitro* and *in vivo* [109]. Surprisingly but photophysical properties of mTHPC remain almost unchanged after the conjugation with AuNPs, probably due to the low loading of mTHPC per NP. The studies *in vitro* demonstrated the potency of mTHPC-AuNPs, namely NPs internalization in human neuroblastoma cells SH-SY5Y and a better PDT effect of conjugates compared with free mTHPC.

It should be also noted that other biomolecules were proposed for conjugation with PSs. For example, the association of PSs with peptides and proteins is recognized as a successful method for enhancing the selectivity and efficacy of photodynamic treatment. Giuntini et al. have already described in the review paper the advances of various peptide-appended porphyrin systems [110].

To date, the focus of investigations is shifted to nanoparticle-based systems, which are non-covalently bound to mTHPC.

3.2. Host-guest supramolecular complexes

Supramolecular systems are one of the most versatile strategies in PS delivery [111]. Initially, in 1999, cyclodextrins (CDs) were proposed only as an approach for mTHPC detection in blood [112] and only in 2016 the first report on CD-based independent delivery of mTHPC was published [42]. Since that time, it has been demonstrated that mTHPC efficiently forms supramolecular non-covalent complexes of few nanometers in size with one or two CD molecules (Figure 4), causing the monomerization of PS molecules in the aqueous surrounding in the presence of CDs [101,112–114]. It should be noted that the complex formation process strongly depends on the type of CD and especially on its substitutes [112,115].

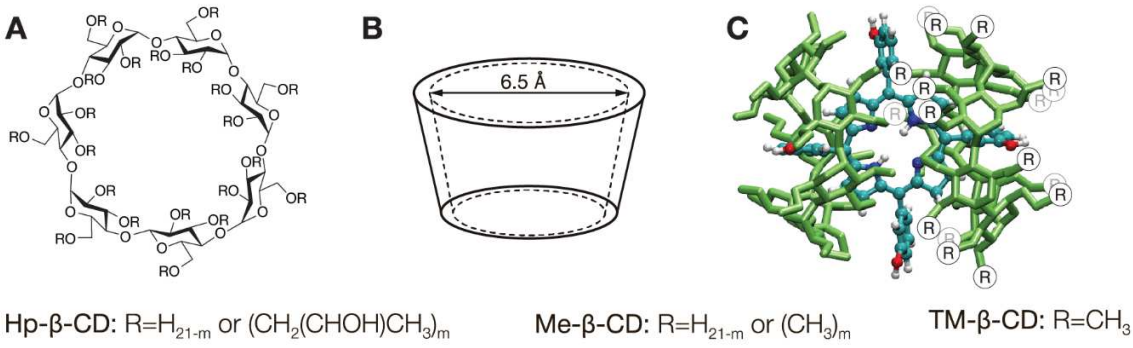

Figure 4. The schematic representation of (A,B) CD structure and (C) inclusion complexes with CDs. Adapted and reprinted with permission from ref [115]

Deep investigations of CDs as pharmaceutical agents demonstrated that depending on the affinity to the drug, the CD could act as a drug solubilizer only (binding constant (K) is less than

10^4 M^{-1}) and/or as drug biodistribution modulator, when K value is higher than 10^5 M^{-1} [116]. In the case of mTHPC, K values are huge reaching 1×10^7 M^{-1} for completely methylated β-CD [115] and as such determining the unique properties of β-CDs as mTHPC nanoshuttles [41,42]. Overall, co-administration of β-CDs/mTHPC complexes could solve several mTHPC drawbacks at once:

1) mTHPC is monomeric from the onset of administration and during the whole circulation time [42]. Additionally, such high affinity allows using CD concentrations as low as 0.5-5 mg kg^{-1} being much lower than toxicity limits (estimated as 40-100 mg/kg and higher) [116]. Even after dilution of complexes in blood, their dissociation resulted in a quick mTHPC redistribution to transport proteins instead of PS self-aggregation.

2) Distribution of mTHPC in serum is modulated by both concentration and type of CD [42]. The presence of a large amount of β-CD results in mTHPC sequestration in inclusion complexes. This also leads to the shift of equilibrium distribution of PS in serum to the inclusion complexes. The high affinity of CDs to mTHPC determines the formation of complexes in serum even in the presence of many potential mTHPC binding sites.

3) The CD-mediated nanoshuttle mechanism for mTHPC offers the opportunity to accelerate mTHPC redistribution between transport proteins themselves and between transporters and cellular membranes (Figure 5A). In the presence of CDs, mTHPC almost completely redistributes between lipoproteins *in vitro* within 30 min [42], while in CD free medium this process takes more than 20 hours [21].

4) Intratumoral mTHPC distribution is improved. CD nanoshuttles accelerate accumulation in tumor cells and strongly improve mTHPC penetration in multicellular tumor spheroids (Figure 5B). This is possibly due to the small size of CD nanoshuttles (1-2 nm), which easily diffuse into the interstitial medium [41]. These observations were confirmed in xenografted tumors *in vivo*, where the maximal level of mTHPC fluorescence from the surface of HT29 tumor

was achieved at already 2 h post-administration of mTHPC/CD complexes [42]. Finally, *ex vivo* fluorescence analysis of isolated tumors at 24 h after injection demonstrated that co-administration of mTHPC with methyl-β-CD increases the total fluorescence signal 1.3 times from isolated tumors compared with free mTHPC (from 196±26 a.u. to 247±30 a.u., $p < 0.05$) [42].

5) Biodistribution of mTHPC is favorably modified [42]. The application of β-CDs decreased the level of mTHPC 1.5–3 times in skin and muscle tissues that together with better PS accumulation in tumor results in the increased therapeutic ratio (tumor/skin or tumor/muscles) up to 2 times (Figure 5C). Moreover, the small size of CDs and strong binding to mTHPC leads to the changes of mTHPC excretion routes: the level of mTHPC in the liver is reduced 1.5 times and increased in kidneys 1.8 times compared to free mTHPC administration.

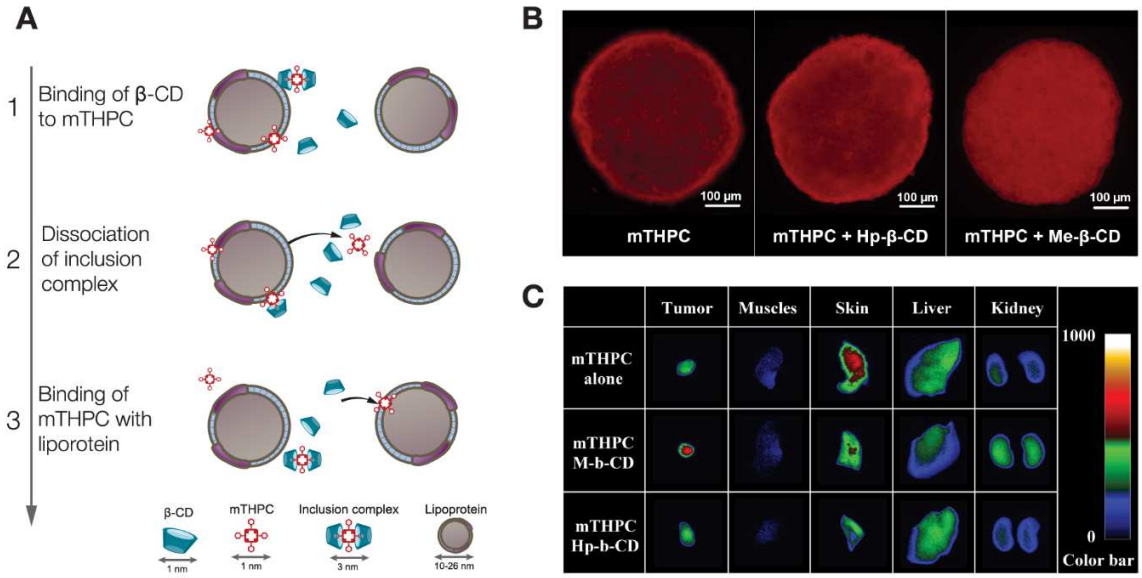

Figure 5. (A) Schematic representation of nanoshuttle mechanism of CD action. (B) Improvement of mTHPC distribution in HT29 multicellular tumor spheroids by CDs. (C) Biodistribution of mTHPC in HT29 tumor bearing mice after co-administration with CDs. Adapted and reprinted with permission from ref [41,42]

Overall, the application of CDs significantly improves the delivery of mTHPC at all stages of PS distribution, making CDs powerful nanocarriers for mTHPC. Further, CDs are supposed not to penetrate into cells [117], therefore they modulate only transportation of PS to the tumor cells keeping intact favorable photobiological properties of PS. Nevertheless, the supramolecular complex lacks long-term stability that together with a strong dependence of CDs effects on their concentration complicates the control of PS delivery at the target site. Moreover, individual application of the supramolecular complex *in vivo* is problematic due to the dilution of CD-mTHPC complexes and a rapid CD excretion from the circulating system after intravenous injection [118].

3.3. Polymeric NPs

To date, macromolecular-based nanocarriers attract the most attention in terms of PS delivery [119]. These nanocarriers possess beneficial advantages, which mainly reside in their excellent colloid dispersity in water enabling solubilization of hydrophobic PS in physiological conditions. Moreover, compared to supramolecular complexes, the size of macromolecular NPs is easily modulated in the nanometer range providing tumor targeting by EPR effect [120]. Although the limitations of EPR are now acknowledged [121], it remains the main process of passive targeting of NPs to tumors. Phospholipids or polymers including FDA-approved synthetic polymers or biopolymers are popular materials for the creation of organic NPs. Polymeric NPs can be formed by self-assembly of biodegradable polymers, which spontaneously assemble into a core-shell structure in an aqueous environment minimizing the system's free energy. Additionally, their surface properties, morphology, and composition can be easily modified to control NP degradation and kinetics of drug release. Next part of this review related to polymeric NPs will be divided into several items according to NP structure: micelles, solid NPs, silica- and protein-based NPs.

3.3.1. Micelles

Micelles are the example of colloidal nanocarriers, micro/nanospheres, polymer-drug conjugates and liposomes [120,122]. Generally, micelles are fabricated based on the self-assembly of amphiphilic blocks or graft co-polymers. The hydrophobic core of micelles can accommodate hydrophobic drugs, whereas their hydrophilic shell ensures the possibility for active targeting or additional protection of NPs with PEG molecules. It is worth noting that polymeric micelles are resistant to dilution effects, for example, they keep initial structure intact upon intravenous administration of the drug formulation due to the very low critical micelle concentration of polymeric surfactants. There are several possibilities to encapsulate hydrophobic drugs, such as physical entrapment to the hydrophobic core and/or covalent binding to the polymer molecules. Still, in the case of mTHPC, the latter may not be preferred due to the significant changes of photophysical properties and uptake limitations. Thus all micellar formulations of mTHPC encapsulate PS within the hydrophobic core (Figure 6).

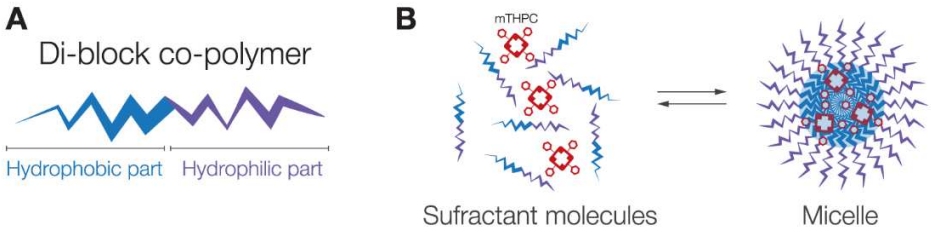

Figure 6. (A) The structure of di-block co-polymers and (B) principal scheme of micelles formation

The evolution of mTHPC micellar formulations includes several stages. In 2008, Hofman *et al.* were the first to report the use of biodegradable mPEG750-b-oligo(ε-caprolactone)$_5$ micelles (10 nm in size) loaded with mTHPC in 15 % (w/w) feed ratio (loading efficacy was 90 %) [43].

However, the authors reported the necessity of site-specific enzymatic micelle degradation and subsequent mTHPC release for effective cellular mTHPC uptake as an explanation of comparable with free mTHPC photocytotoxicity in 14C cells. That is why in 2017 they proposed the updated mTHPC-loaded micelles as an approach to treat atherosclerotic lesions using PDT modality [49]. The next step was to change the mechanism of mTHPC release in order to increase the accumulation of PS for efficient PDT. It has been proposed to use pH-responsive poly(2-ethyl-2-oxazoline)-*b*-poly($_{D,L}$-lactide) (PEOz-*b*-PLA) as well as poly(ethylene-glycol)-methacrylate-co-2-diisopropylamin (PEGMA-co-DPA) di-block co-polymers in micelles formation to achieve control drug release at the tumor site [45,46]. The obtained micelles were about 100 nm in size (77 nm for PEOz-*b*-PLA and 140 nm for PEGMA-co-DPA) and possessed a high loading efficiency (a percentage of drug loaded in NP) of mTHPC (92.5 % and more than 80 % for PEOz-*b*-PLA and PEGMA-co-DPA, respectively). It was hypothesized that NP with such size will passively target tumor and that mTHPC will be released in the tumor microenvironment, which is characterized by low pH 5.0. However, despite not optimistic *in vitro* results [45,46], in HT29 tumor bearing mice, the authors demonstrated reduced skin photosensitivity of micellar mTHPC formulation alongside with the similar to free mTHPC antitumor PDT efficiency. The successful PDT using micellar mTHPC was achieved in the case of integrin-rich U87MG tumors [47]. Using the mixture of chitosan-vitamin E succinate conjugates and D-α-tocopheryl-PEG conjugates grafted with cyclic RGD peptide Wu and co-workers prepared 145-nm micelles and loaded them with mTHPC with a loading efficiency 50 %. Such active targeting improved accumulation and PDT efficiency in monolayer cells and increased mTHPC penetration depth in multicellular tumor spheroids *in vitro*, while *in vivo* RGD-modification resulted in inhibition of the growth of U87MG tumors without any toxicity to other tissues.

Recently, the concept of polymeric micelles was updated with new amphiphilic DNA-based co-polymers [123]. Thus, Liu and co-workers efficiently incorporated mTHPC in 11-nm lipid-DNAs micelles (loading capacity 11.7 %, w/w) [48]. *In vitro* studies demonstrated better biocompatibility and reduced dark toxicity of mTHPC loaded lipid-DNAs micelles in various cell lines compared with free mTHPC. However, a high loading capacity in DNA-based micelles also has a negative aspect consisting of concentration quenching [48], determining the dependence of PDT efficiency of DNA-based micelles on drug release processes. Immunogenicity of DNA-based micelles was not addressed in this study. An interesting perspective could be offered by the bare DNA self-assembly NPs. Indeed, the previous research on these NPs demonstrated a low level of their immunogenicity, indicating the biosafety of DNA-based materials [124].

3.3.2. Solid polymeric NPs

Solid polymeric nanospheres are defined as colloid stable nanostructures. Such NPs consist mainly of biocompatible and biodegradable components exhibiting controlled drug release through biodegradation after the intracellular accumulation of NPs. Depending on the type of polymers, various size of nanospheres could be obtained, *i.e.* ultrafine 2-3 nm polyacrylamide NPs [50], 145-nm poly-($_{D,L}$-lactide-co-glycolide) (PLGA) NPs [52], polyplex NPs based on chitosan (ca 498 nm) or chitosan oligomer lactate (ca 728 nm) polymer [125]. The opportunity to synthesize ultrafine NPs for mTHPC delivery was used by Gao De and co-authors [50]. The authors supposed that these NPs could be of interest *in vivo* due to their ultrasmall size and potential low protein and macrophage adsorption. To date, *in vitro* studies demonstrated PDT cytotoxicity in C6 rat glioma cells.

The most common polymer used for solid NPs preparation is PLGA. Owing to excellent biocompatibility and biodegradability, PLGA has been approved by the US Food and Drug Administration (FDA) [126]. After cellular uptake, it undergoes hydrolysis generating two monomers (lactic acid and glycolic acid) with very low systemic toxicity. Therefore, in 2011 Low and co-workers proposed PLGA-based nanospheres as an mTHPC delivery system. With this aim, they synthesized PLGA nanospheres of 283.2 ± 20.4 nm and tested their efficiency against HT29 monolayer cells and multicellular tumor spheroids [51]. PLGA nanoparticles successfully delivered mTHPC to HT29 cells, released it into the cytoplasm and caused apoptosis after illumination. However, no further changes in PS accumulation and distribution in both monolayer and spheroid models were observed compared with free mTHPC, probably because of untimely release. Photocytotoxicity in monolayer cells was also comparable with free mTHPC. To prevent adverse interaction of PLGA NPs with proteins and mononuclear phagocytic system, PEGylation of NPs was performed [52,53]. Depending on the preparation technique, the particles from 100 to 170 nm were obtained and loaded with mTHPC. PEGylated mTHPC-PLGA nanospheres were sufficiently stable in serum over the observed time frame [53]. Nevertheless, PEG shell is also the hydrophobic environment and may bind mTHPC, therefore substantial leak of the drug may occur in the presence of serum proteins [52]. Concerning *in vitro* efficiency, PLGA-mTHPC-NPs with PEG shell displayed similar behavior as ultrafine nanospheres. Finally, the study of mTHPC biodistribution upon its delivery by PLGA NPs demonstrated similar to Foscan® tumor selectivity raising the question on the possible improvement of PLGA platform with active targeting molecules or stimuli-response moieties. Recently, PLGA-nanospheres were upgraded using light-degradable aliphatic polycarbonate moieties for the controlled release of mTHPC [127]. To date, no *in vitro* data on the interaction of synthesized NPs with cells are available, however, the proposed NPs are activated at

365 nm suggesting significant limitations of its *in vivo* application due to the small penetration depth of UV light.

Along with the conventional materials for polymeric NPs as PLGA, some specific nanomaterials were applied such as chitosan polymer or chitosan oligomer lactate [125]. These natural biodegradable polymers are nontoxic, biocompatible, biodegradable, can be easily chemically modified, have a relatively low cost and certain flexibility to respond to pH changes [128]. Thus, chitosan polymer or chitosan oligomer lactate were used for the preparation of biodegradable polyplex nanospheres [125]. These NPs possessed the size of more than 300 nm and at pH = 5.0 they were unfolded increasing in size up to 500 nm. However, as many strategies, such NPs passed only the basic release experiments, so additional *in vitro* and *in vivo* experiments are needed to assess the applicability of natural biodegradable nanospheres in mTHPC-PDT.

3.3.3. Silica-based NPs

Silica-based NPs (SiNPs) represent porous nanospheres which can be loaded with organic molecules by covalent links to the silica matrix or by simple entrapping as in the case of hydrophobic mTHPC. SiNPs are transparent to light and photochemically inert. The first studies on mTHPC-SiNPs were performed by Yan and Kopelman in 2007 [129]. The authors hypothesized that SiNPs may decrease mTHPC photodegradation and further demonstrated the reasonable generation of singlet oxygen by 180-nm mTHPC-SiNPs. However, this approach works only when entrapped mTHPC is delivered to cells in association with the silica matrix. As was mentioned above, the drug release mechanism is usually essential for such nanoplatforms, nevertheless, the balance is needed. For example, SiNPs were organically modified to deliver mTHPC to human oesophageal squamous carcinoma KYSE 510 cells [54]. The authors successfully entrapped mTHPC in feed ratio of 1 %

(w/w) into 41-nm organic-modified SiNPs (ORMOSIL NPs). However, without PEG coating, mTHPC is completely released from ORMOSIL to serum proteins in 1 hour making NPs inefficient as nanocarriers. Silica NPs with delayed mTHPC release demonstrated PDT potency *in vivo* in MDA-MB-231 – bearing Nu/Nu mice compared with conventional mTHPC formulation Foscan® [56]. Moreover, the authors reported that mTHPC-loaded SiNPs could pass through the blood-brain barrier [56], as was already demonstrated for PEGylated SiNPs [130,131], perhaps, due to the receptor-mediated endocytosis by the endothelial cells of the brain capillary followed by transcytosis and specific-transporters support [132]. Based on that, the authors suggested SiNPs as a potent delivery system for mTHPC against brain metastases [56].

In fine, silica-modified calcium phosphate NPs were used as a multifunctional theranostic platform that regroups near-infrared fluorescence optical imaging with optimized tumor targeting and PDT. With this aim, Haedicke and co-workers embedded mTHPC into synthesized 200-nm CaP/PEI/SiO_2 and attached near-infrared fluorescence agent DY682 along with RGDfK-peptide for active targeting of CAL-27 tumor (Figure 7) [55]. SiNPs-RGD loaded with mTHPC were selectively accumulated in the tumor tissue *in vivo* (Figure 7B). PDT with these NPs was rather efficient (75% of cured mice) (Figure 7C). In addition, the authors demonstrated PDT-induced damage of tumor vasculature using IRDye® 800CW RGD and detected apoptotic tumor cells already 2 days post- PDT (Figure 7D).

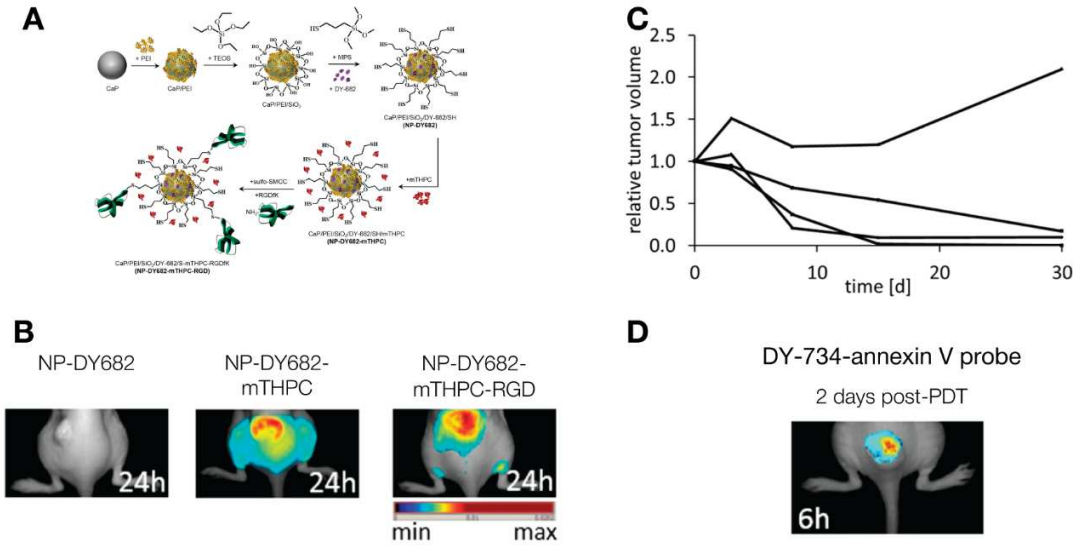

Figure 7. (A) Schematic representation of RGDfK-conjugated silica-modified calcium phosphate NPs loaded with DY682 fluorescent dye and mTHPC. (B) The representative composite images illustrate the fluorescence of the NPs in mice bearing CAL-27 tumors at 24 h after injection. (C) The kinetics of relative volume of CAL-27 tumors (related to the volume before PDT) in mice after nanoparticle-based PDT (n = 4). (D) Representative composite image showing the fluorescence of DY-734-annexin-V in CAL-27 tumor-bearing mice at 2 days after PDT with mTHPC-SiNP-RGD. Adapted and reprinted with permission from ref [55].

3.3.1. Protein-based NPs

Protein nanoparticles have better biocompatibilities, biodegradability, non or low - antigenicity and thus could be also attractive material for drug delivery platforms [133]. For instance, human serum albumin (HSA) is one of the most known natural transporters of PS in serum [134] and has been proposed for the preparation of protein-based nanocarriers for PSs. mTHPC molecules, however, possess low affinity to HSA binding sites [21], thus mTHPC encapsulation requires chemical cross-linking of HSA to obtain porous NP structure (Figure 8). Chemical cross-

linking of HSA units results in the formation of 150-200 nm porous NPs [57,135]. Such microenvironment is supposed to induce non-covalent adsorption of drug molecules to the surface of HSA and can be altered by varying the cross-linking degree between HSA units as was performed for mTHPC [58]. *In vitro* studies of mTHPC-HSA NPs on Jurkat cells demonstrated efficient intracellular accumulation and similar to free mTHPC total phototoxicity. The *in vivo* potency of HSA-NPs is questionable, however, the opportunity to adjust drug release and size by varying cross-linking degree makes such platforms very flexible.

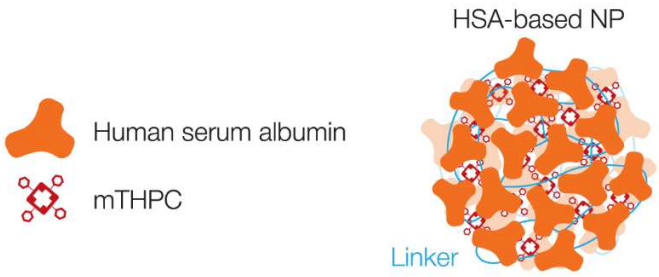

Figure 8. Schematic representation of HSA-based mTHPC NPs.

3.4. Lipid-based NPs

In the range of natural biomaterials, lipids as one of the main components of biological membranes and lipoproteins as serum transporters are particularly attractive. Lipid-based drug delivery systems have shown effective size-dependent properties together with a high degree of biocompatibility and versatility [136]. Moreover, lipid-based NPs should be very capacious due to the high affinity of mTHPC to lipid microenvironment. Finally, phospholipids are major components of biological membranes and could be easily incorporated in membrane structures providing required drug release upon the fusion with biomembranes. In the next chapters, we shall

review several types of lipid-based NPs used for mTHPC delivery, including vesicular (liposomes and extracellular vesicles) and solid lipid nanoparticulate systems.

3.4.1. Liposomes

Among various lipid-based formulations, classical "liposomes," which primarily consist of phospholipids (basic components of cellular membranes) were extensively studied as mTHPC nanocarriers [137]. Liposomes represent bilayered phospholipid nanocapsules which could be loaded with hydrophobic compounds in the lipid bilayer (Figure 9). Liposomes could contain a lot of mTHPC molecules in the monomeric state without destabilization of the lipid bilayer (up to 1:13 drug to lipid ratio) due to the hydrogen bonding between lipids and mTHPC molecules [138]. Biolitec AG (Jena, Germany) proposed a commercial mTHPC liposomal formulation Foslip® which is based on the conventional dipalmitoylphosphatidylcholine (DPPC) liposomes (*ca* 120 nm) with the addition of 10 % negative charged dipalmitoylphosphatidylglycerol (DPPG) lipid to the bilayer for colloidal stability [139]. After two decades of investigation, we can state that Foslip® is one of the most successful and the most studied mTHPC nanoformulation. Since the first report in 2005, over 25 papers have been published reporting various aspects of Foslip® characterization and application in mTHPC-PDT (Table 1).

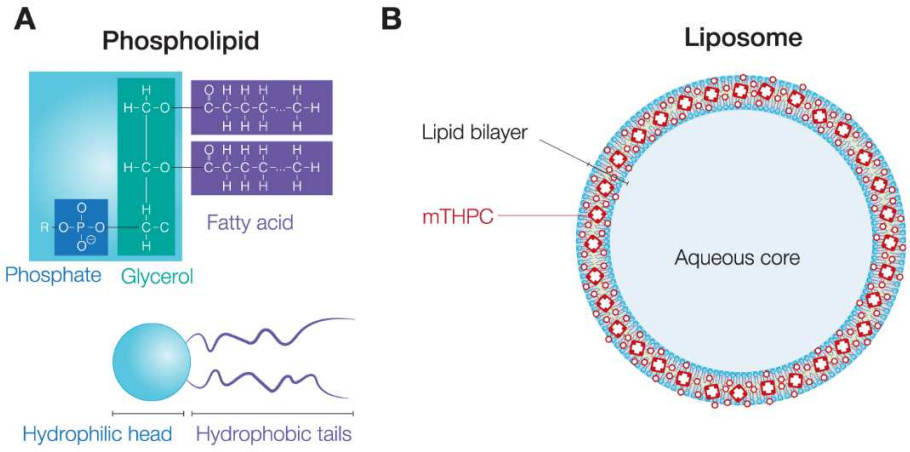

Figure 9. (A) Chemical structure of phospholipids and (B) schematic representation of mTHPC-loaded liposome.

Briefly, liposomes were successfully internalized into cellular membranes ensuring efficient mTHPC accumulation in many types of cancer cells [24,63,66,73,75]. After internalization, the liposomal membrane is simply fused with cellular membranes and mTHPC is redistributed between cellular compartments. Thus, no apparent difference in intracellular localization of Foslip® and free mTHPC was observed. The most important is that Foslip® overcomes almost all drawbacks of free mTHPC during its biodistribution, namely:

1. Lipid microenvironment provides complete monomerization of mTHPC during all stages of its distribution *in vivo* [59,61,64]. Moreover, Foslip® is administrated in the water-buffer solution thus reducing the pain and negative effects upon injection.
2. Foslip® demonstrated higher bioavailability [67] and tumor selectivity than free mTHPC at shorter post-injection times [61,68]. Indeed tumor-to-muscle ratios were up to 9 already after 15 h post-administration compared with 24h and more for Foscan® [70]. Significant selectivity of Folsip® between the lesion and normal surrounding skin at 4 h was observed in a non-melanotic skin tumor model [60]. Moreover, application of liposomal mTHPC formulations

decreased dark cytotoxicity, keeping high phototoxicity of mTHPC *in vitro* [24,66,73] and thus providing the opportunity to decrease general post-PDT photosensitivity.

3. Foslip® showed appropriate PDT-efficiency in xenografted tumor models [70,74,75,81]. It was observed that PDT at very short (1-3 h) drug-light-intervals (DLIs) induces persistent oedema, significant ectoderm hyperplasia and a decreased vessels density *in ovo* in xenografted chick embryo chorioallantoic membrane model [69]. In the case of xenografted mice, DLIs of 6 h and more were effective in terms of growth delay [64,70].

Additionally, Foslip® was successfully applied in a low-dose PDT treatment. Foslip®-based PDT-induced photoimmunomodulation resulted in a considerable acceleration of wound healing [65]. Moreover, low-dose Foslip®-PDT demonstrated promising results as a treatment modality to prevent colitis-associated carcinogenesis in a murine model of ulcerous colitis [72].

Nevertheless, liposomes still present some unsolved drawbacks. In fact, due to their big size and lipid composition, tumor cells internalize liposomes either by fusion or by one of the endocytosis mechanisms [140]. These factors significantly limit the penetration of mTHPC loaded in liposomes across the tumor tissue as was observed in multicellular tumor spheroids *in vitro* [73,76,77]. Inhomogeneous distribution of mTHPC in tumor can result in relapse of tumor growth *in vivo* [71], and was even observed after intratumoral *in vivo* administration of Foslip® [62]. Additionally, intravenously administrated liposomes are rapidly disintegrated in blood upon the interaction with serum components releasing almost all PS [70,141]. Thus, after 6 hours post-administration, only 40 % of intact liposomes remain in plasma. It is worth noting that liposomes destabilization is mainly the result of lipid transfer between lipoproteins and lipid vesicles. This transfer is also accompanied by redistribution of PS to serum proteins [141–144]. Due to both the release and liposome destruction, Foslip® pharmacokinetics after already 6 h post-administration reflects the circulation of free mTHPC released from the liposomes [70].

Sterically protected PEG-modified liposomal formulation mTHPC, Fospeg® (Biolitec Pharma Ltd., Jena, Germany), was proposed to overcome the destruction of liposomes and to increase a plasma half-life. Foremost, Fospeg® exhibited the absence of carrier destruction and due to the PEG steric protection, a significantly higher amount of mTHPC remains in liposomes compared to Foslip® [70]**.** Fospeg®, as well as Foslip®, demonstrated reduced dark cytotoxicity effects in monolayer cells *in vitro* [79,80,82]. Additionally, incorporation of mTHPC into long-circulating PEGylated liposomes provided a high tumor selectivity and accumulation even at 4 hours post-injection compared with 24 hours for Foslip® or Foscan® [64,70,78,81,83]. As such, PDT efficiency with Fospeg® was determined as maximal for short DLIs (15 h) and this is the main advantage of sterically stabilized liposomes compared with non-pegylated Foslip® [70,78,83]. Therefore, Pegaz and co-authors proposed Fospeg® as a potentially suitable compound for obtaining more selective killing of choroidal neovasculature for age-related macular degeneration with PDT. Moreover, recent studies related to photodynamic treatment of multidrug-resistant cells suggested that Fospeg® could be used to overcome MDR1-related cancer drug resistance [84]. It should be noted that similar effect was also demonstrated for free mTHPC [145]. Nevertheless, the steric protection does not solve the problem of liposome penetration in tissue making it even worse [73]. It was demonstrated that in the case of Fospeg® up to 30 % of encapsulated mTHPC molecules are localized in the PEG shell with easy access to acceptor structures (i.e. serum proteins) [141]. Thus, both Fospeg® and Foslip® showed a major efflux of mTHPC from liposomes in the circulation [141,146].

To overcome low percutaneous penetration in the case of topical mTHPC delivery for the cutaneous malignant (basal-cell carcinoma) or non-malignant diseases (psoriasis, acne, etc), flexible liposomes were suggested [89–91]. The authors reported that the addition of ethanol and terpene (invasome) or Tween® 20 (flexosome) into the lipid bilayer makes it flexible and provides a

significant enhancement of mTHPC accumulation in the skin compared with conventional liposomes in preclinical models [89–91]. It was found that the highest penetration ability of mTHPC in stratum corneum and deeper skin layers are achieved for cationic flexosomes.

It is worth noting that there were already the attempts to vary the lipid composition of liposomes for mTHPC delivery. The cationic liposomes from dimyristoylphosphatidylcholine (DMPC) containing Gemini surfactant were proposed as a promising tool to overcome the blood-brain barrier and to improve mTHPC delivery to glioblastoma cells [85–88].

In fine, despite the success of liposomal formulations *in vivo*, their translation into clinical practice is limited perhaps due to the not optimal drug release and limited penetration of drug-loaded liposomes into the tumor tissues. In order to maximize the benefits of liposomal carriers, a balance between drug delivery to the tumor and drug release from the liposomes must be achieved, for example using stimuli-response moieties, making the liposomal carries triggerable.

3.4.2. Extracellular vesicles

While liposomes represent pure lipid bilayer, natural biomembranes consist of a mix of different lipids including peptides, saccharides, receptors, etc. All these components confer membranes' flexibility, providing specific cell-recognition mechanisms and protecting bilayer from undesirable interactions with other biomacromolecules [147]. Thus, it was suggested to use natural liposomes, derived from the cellular membranes, namely extracellular vesicles (EVs), as nanocarriers for PSs [148], including mTHPC [77,92,98]. To encapsulate mTHPC in EVs, precursor endothelial cells were loaded with mTHPC before EVs isolation [77]. As a result, the purified EV suspension was loaded with 3 % mTHPC and was slightly heterogeneous in size (from 100 to 500 nm). To increase the loading capacity of mTHPC into EVs, EVs were modified by fusion with mTHPC-loaded liposomes [92]. This approach has allowed increasing the drug encapsulation

efficiency up to 90 %. In addition, due to the biogenic composition, mTHPC-EVs showed a remarkable increase in stability in the presence of plasma proteins compared with conventional liposomes as Foslip® [77]. Upon the interaction with serum components, EVs kept their integrity, while its size was reduced to 70 nm. In its turn, the small size of serum-treated EVs together with enhanced flexibility of natural membrane caused deep penetration of EVs-based mTHPC into tumor spheroids. It is worth noting that EVs also release mTHPC in the presence of serum but much slower than Foslip® [77]. The opportunity of mTHPC release from EVs promotes PS accumulation. Indeed, the cellular uptake and photocytotoxicity of mTHPC-EVs were 2 and 4-times higher in 3D tumor spheroids than Foslip® and free mTHPC, respectively. EVs were also used as a theranostic platform, loaded simultaneously with iron NP for diagnosis and mTHPC for therapy [97,98]. Intratumor administration of these NPs showed improved PDT efficacy *in vivo* extending a tumor growth delay. To date, EVs is a novel perspective liposomal-based delivery nanoplatform which requires additional studies to fully explore its benefits for drug delivery.

3.4.3. Solid lipid NPs

Solid lipid nanoparticles (SLNPs) are aqueous colloidal dispersions, their matrix is composed of solid biodegradable lipids [149]. While vesicular lipid-based mTHPC formulations consist of the bilayer only, which is only a small volume of NP, a greater part of SLNPs' volume consists of lipids thus providing the opportunity to encapsulate higher amount of hydrophobic PS molecules [150]. Usually, lipid core is coated with polymeric compounds such as PEG to prevent the dissolution of lipid NPs and a fast drug release in biological fluids. The first report on nTHPC-SLNPs was performed in 2000 when 190-nm oil (Miglyol) reservoirs with PLA-PEG or PLA coated with poloxamer 188 external layers were loaded with mTHPC [44]. However, the choice of polymeric shell had a negative impact on the internalization of NPs and also on PDT efficiency *in vitro*. Then, 14 years later instead of biodegradable PLA, phospholipids (lipoid s75) and

pegylated surfactants (Myrj s40) were suggested to coat lipid inner core (soybean oil and Suppocire NB) (Figure 10) [93]. The authors called it Lipidots and tested this mTHPC-based formulation in various tumor models [74,94,151]. Varying the ratio between components (oily phase : PEG surfactant : phospholipids), the size of Lipidots could be modulated from 20 to 120 nm providing the opportunity to find out the best composition for mTHPC delivery. In advanced 3D cell culture model, the authors demonstrated that small 50-nm Lipidots possess both higher accumulation and penetration ability compared with 120-nm ones. Nevertheless, PS distribution in spheroids, as well as PDT efficiency of 50-nm Lipidots, were close to free mTHPC. A similar tendency was also observed in a CAL33 tumor model in mice. The treatment with conventional liposomal formulation Foslip® was significantly superior to both Foscan® and Lipidots. Thus, the authors emphasized the biocompatibility of Lipidots as the main benefit of this formulation.

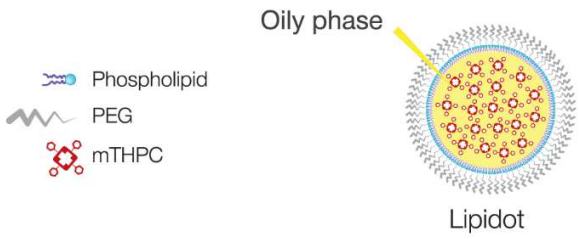

Figure 10. Schematic representation of mTHPC-loaded Lipidots. Adapted and reprinted with permission from ref [94].

In 2016, Brezaniova with co-workers presented liquid droplets based on lipid core stabilized by the nontoxic polymeric surfactant co-polymer poly(ethylene oxide-block-e-caprolactone) to deliver mTHPC [95]. Even without active targeting, the obtained 30-nm NPs efficiently delivered mTHPC to the target cells resulting in a 2-fold increase of photocytotoxicity in 4T1 and human

breast carcinoma MDA-MB-231 cell lines. *In vitro* experiments also demonstrated high stability in the serum of mTHPC encapsulated in NPs. The success of formulation *in vitro* was also accompanied with more striking and large necrotic areas compared with Foscan® after PDT in xenografted human breast carcinoma MDA-MB-231 mice. Foremost, the significant advantage of mTHPC loaded SLNP is a considerable decrease in DLI (3 h) with 100 % tumor growth inhibition at 3rd day post PDT; nevertheless, the partial tumor relapse on the periphery of the original tumor occurred 35 days after PDT.

Recently, several studies involving mTHPC excitation through fluorescence resonance energy transfer (FRET) from the components of the nanodelivery system were reported. The first study was conducted in 2015, when 13–48 nm SLNPs coated with semiconducting polymers and PEGylated phospholipids demonstrated efficient generation of singlet oxygen by mTHPC upon FRET after excitation of semiconducting polymers at 600 nm (Figure 11) [152]. However, one can suppose that tumor cells can internalize the NPs without the release of mTHPC. Further, the irradiation at 600 nm *vs* 650 nm is not beneficial for mTHPC-PDT. Probably, this is the reason why up to moment there are no available *in vitro* and/or *in vivo* data.

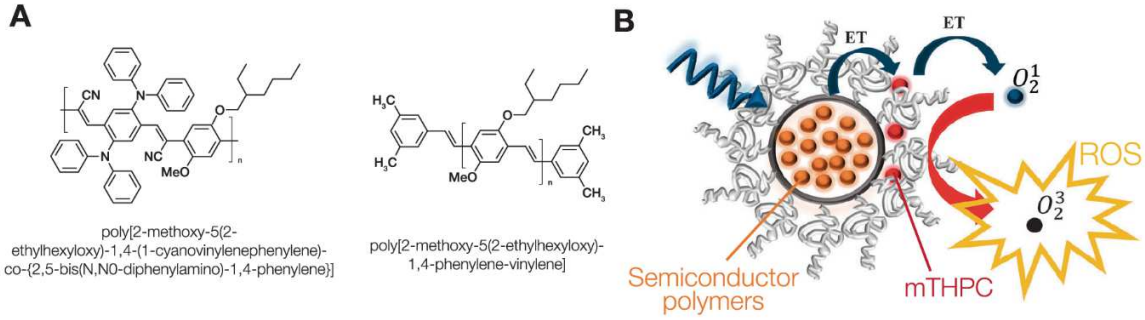

Figure 11. (A) Chemical structures of semiconductor polymers. (B) Semiconducting polymer dot enhances the singlet oxygen production by FRET to the PS. Adapted and reprinted with permission from ref [152].

3.5. Carbon nanotubes (CNTs)

The strategy to use semiconductor materials as components of nanoplatform for mTHPC delivery was introduced recently with CNTs. Semiconducting CNTs generate heat under illumination in a wide spectral range demonstrating an intrinsic photothermal effect [153]. Marangon and co-workers constructed a nanosystem based on multi-walled carbon nanotubes (MWCNTs) loaded with mTHPC using π-π stacking on their surface for cancer treatment by the combination of photodynamic and photothermal therapies [96]. MWCNTs were shortened to increase their water dispersibility and therefore they obtained the size of 39 nm in diameter and 400 nm in length. mTHPC was loaded with a maximum loading of 3.5%wt resulting in a complete quenching of mTHPC emission by nanotubes. According to this, PS is inactivated in the complex with MWCNTs outside the cell and becomes active after cell internalization of the complex and subsequent light irradiation. The authors evidenced different routes of apoptosis in human ovarian tumor cells (SKOV3) depending on the irradiation conditions culminating synergistically in the apoptosis of the whole cell population when combined PDT and photothermal treatment was applied. Nevertheless, the behavior of such complex in blood raises the questions on the bioavailability and selectivity of MWCNTs as well as on the rate of mTHPC released to serum components.

3.6. Hybrid nanodelivery systems

Nanocarriers mainly improve particular mTHPC drawbacks modifying PS behavior at one of the stages of its distribution in the organism. All NPs prevent mTHPC aggregation, while only a few of them improve selectivity and enhance penetration of PS into tumor tissue. In order to maximize the improvement, hybrid nanodelivery systems, which are based on a combination of individual

carriers were suggested as an advanced strategy for mTHPC delivery. Thus, a smart choice of hybrid system components could provide a synergetic effect, making mTHPC delivery efficient at all stages.

Due to functional versatility of liposomes, the first example of hybrid system was based on the liposomes which include mTHPC in lipid bilayer while magnetic iron oxide NPs were encapsulated in the inner aqueous core (Figure 12) [99]. The double cargo was translated into double functionality with photogeneration of singlet oxygen and heat production upon alternating magnetic field stimulation, thus coupling PDT with magnetic hyperthermia (MHT). As a basis, pegylated liposomes (such as Fospeg®) were taken with a slight modification of lipid composition. The authors successfully loaded 200-nm lipid vesicles with mTHPC (the lipid-to-drug ratio was about 7) and iron oxide NPs (about 2400 NPs per vesicle). The authors proved *in vitro* efficacy of such hybrid NPs as PDT agents as well as MHT sensitizers. *In vivo*, each treatment alone was able to inhibit tumor growth, while the combination of both therapies remarkably led to the complete tumor regression.

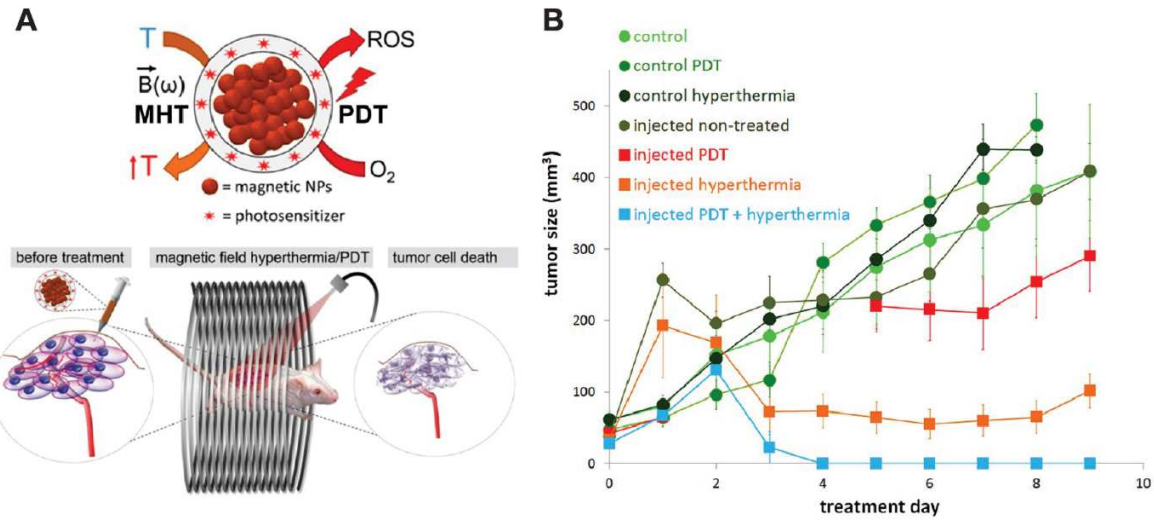

Figure 12. (A) Schematic description of ultramagnetic photosensitive liposomes structure and therapeutic strategy. (B) Tumor growth curves of different control groups and treatment groups. Adapted and reprinted with permission from ref [99].

Similar idea to combine hyperthermia and PDT was recently reported by Tsai and co-workers [100]. Instead of liposomes, a concept of SLNPs was adapted for synergistic treatment of glioblastoma using the combination of photothermal (IR-780) and mTHPC-mediated photodynamic actions (Figure 13). Hybridization aimed to a use oleic acid-coated upconversion NPs (UCNP) as a basis of solid lipid core due to their ability to excite mTHPC though FRET mechanism absorbing near-infrared light (980 nm). Along with near-infrared excitation, the treatment of brain tumors requires penetration across the blood-brain barrier. For this purpose, the PEGylated surface of hybrid NPs was decorated with angiopep-2 as an active targeting agent. The concept was successfully confirmed on astrocytoma ALTS1C1 cells *in vitro* demonstrating pronounced cytotoxicity by combined NIR-triggered photodynamic and photothermal therapies. In consistence with the increased penetration of NPs through endothelial monolayer *in vitro*, the NPs also demonstrated selective accumulation in brain tumor and prominent apoptotic and necrotic effects on orthotopic tumors *in vivo* after dual phototherapies (median survival was 24 days). All reported data converge on the idea that proposed NPs are a promising tool against glioblastoma.

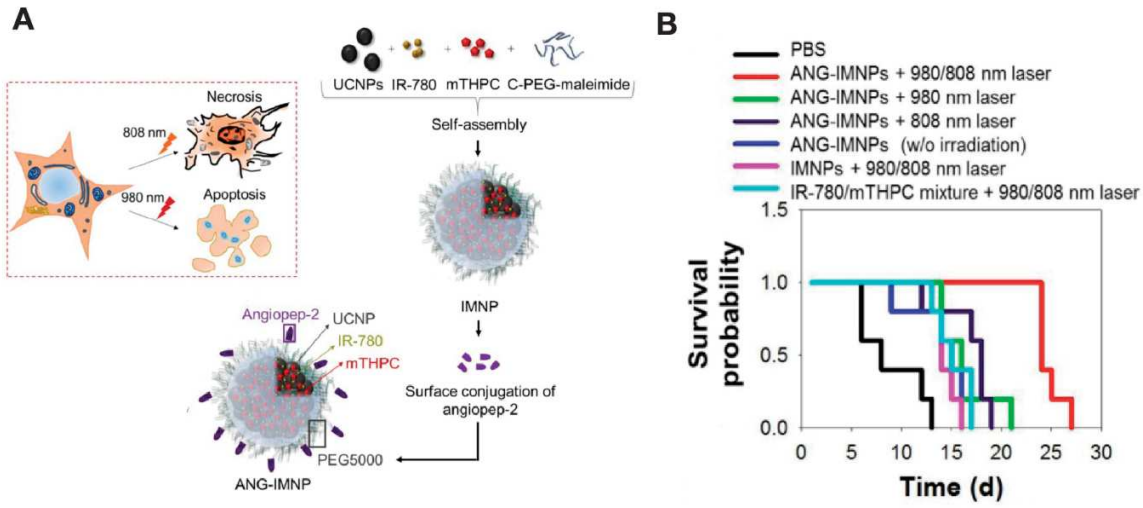

Figure 13. (A) Schematic representation of hybrid NPs structure and the mechanisms of cancer cell necrosis and apoptosis induced by hybrid NPs with 980/808 nm laser irradiation. (B) Kaplan-Meier survival curves of the glioma-bearing mice (n = 5). Adapted and reprinted with permission from ref [100].

It should be noted, that the development of the described hybrid system was focused on the combination of treatment modalities, while the delivery aspects were sometimes neglected. Recently, "drug-in-cyclodextrin-in-liposome" (DCL) hybrid NP was proposed to deliver mTHPC (Figure 14) [76]. It is worth noting that this approach has been firstly announced by McCormack & Gregoriadis [154] aiming an increase of encapsulation efficiency of hydrophobic drug in liposomes. Due to the unique properties of mTHPC/CDs inclusion complexes, this concept got a second wind. We suppose that liposomes could act as a container while its rapid release and degradation in the biological medium could stimulate the transportation of mTHPC/CD, encapsulated in the aqueous core of liposomes. Moreover, the released mTHPC/CD complexes additionally may increase mTHPC tumor selectivity and improve its penetration into tumor tissues completely refining

mTHPC biodistribution. The optimization of drug-loading procedure allows stable and efficient encapsulation of mTHPC bound to β-CDs into conventional liposomes [76]. The synthesized 135-nm mTHPC-DCLs demonstrated a complete penetration of mTHPC and homogeneous PS distribution across the multicellular HT29 tumor spheroids *in vitro* (Figure 14 B&C). However, hybrid mTHPC-DCL construct should be additionally optimized for *in vivo* studies expecting critical improvements of mTHPC biodistribution in tumor compared to its liposomal counterparts (Foslip®).

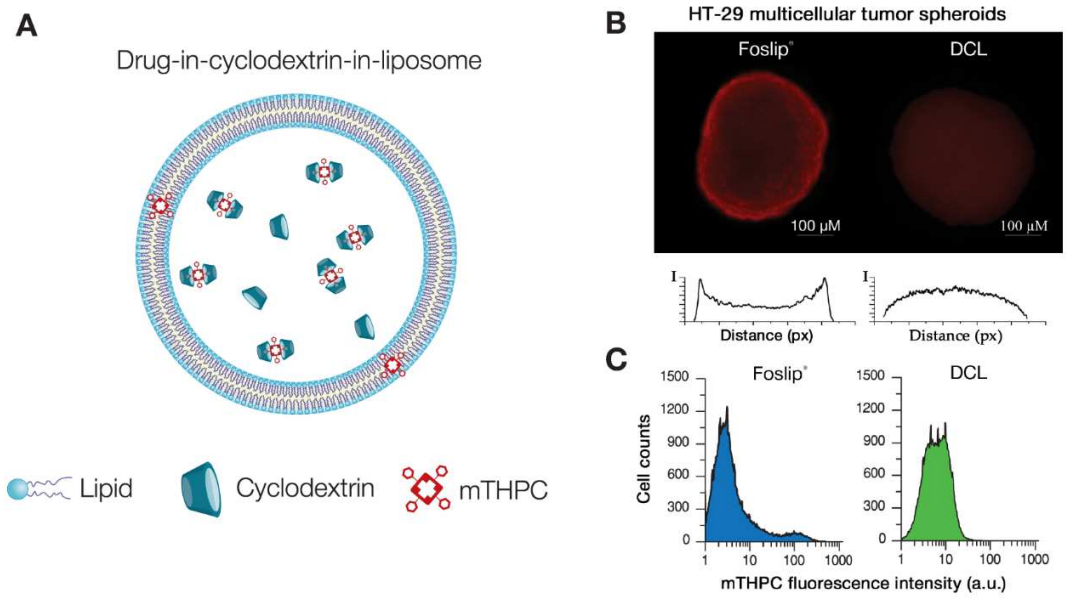

Figure 14. (A) Schematic representation of the mTHPC-DCL hybrid NP. Improvement of mTHPC distribution in HT29 multicellular tumor spheroids by DCL: (B) fluorescence imaging and (C) flow-cytometry analysis. Adapted and reprinted with permission from ref [76].

4. Conclusions and Perspectives

The rapid growth of nanotechnology is one of the most quickly emerging tendency in cancer therapies, including PDT. Nanotherapeutics are supposed to overcome the major constraints of

conventional medicine such as low solubility and stability, non-adequate pharmacokinetic profiles and side effects. To date, many nanoplatforms were applied for the delivery of mTHPC, one of the most potent clinically approved PS.

Potent mTHPC-based NPs have been intensively tested in different *in vitro* preclinical models (2D and 3D tumor cell cultures), while complete PDT studies, including biodistribution, pharmacokinetics and PDT efficacy in tumor-bearing *in vivo* animal models are rather sparse. This situation seriously complicates the assessment of the benefits of mTHPC-based NPs against Foscan®. We attempted to summarize the general benefits and limitations of mTHPC-based nanoconstructs compared to free mTHPC (Table 2). In spite of the great disparity of pros and cons for each nanoconstruct, some common elements can be discerned. First of all, nanoplatforms effectively solve the problem of mTHPC aggregation, providing easy administration of PS. Secondly, the dark toxicity of mTHPC delivered by NPs is significantly lower than that of free drug. Further, among mTHPC nanoformulations that were tested in preclinical *in vivo* models, the majority of them demonstrated an improved selectivity and bioavailability. Common drawbacks for mTHPC-based NPs are difficult to list since they greatly depend on individual characteristics of each NP. We can only note a rather poor drug release at the target site. It seems inconsistent but NPs with high stability in plasma lack the efficient drug release at the target tumor site. An optimal balance between NPs' plasma stability and efficient PS release could be achieved with the tailoring of stimuli-response moieties thus providing control drug release.

Due to the variability of processes involved in the drug distribution at various stages (blood circulation, tumor tissue distribution, intracellular accumulation), the algorithms for the design of ideal NPs do not yet exist. We suppose that combining different NPs in one nanoplatform will foster future research avenue in the field of mTHPC delivery. Lipid and polymer nanocapsules could be used for this purpose. To date, several reports on the successful inclusion of various drug-loaded

nanoparticles (CDs complexes, micelles) in liposomes [155,156] or inclusion of drug-CDs complexes in PLGA nanocapsules [157] have been published. Recently, hybrid drug-in-cyclodextrin-in-liposome nanoplatform was adapted for mTHPC combining the benefits of both liposomal nanocarriers and CD nanoshuttles [76]. Finally, the association of different nanoparticles in one nanoplatform allow the combination of several treatment modalities improving anti-tumor effect *in vivo* and offering an advanced strategy of anticancer treatment [158].

Table 2. The benefits and limitations of nanoplatform-based delivery against free mTHPC

Benefits	Limitations
Conjugates	
• Drug solubility • Lower dark phototoxicity *in vitro* • Prolonged plasma life-time *in vivo* • Better selectivity *in vivo*	• Modification of chemical structure of PSs • Hurdles in uptake in tumor cells *in vitro* • Active targeting is limited by low loading capacity (several PS molecules)
Inclusion complexes	
• Drug solubility • Alteration of distribution in serum • Accelerated uptake to the cells *in vitro* • Improved penetration in tumor tissue *in vitro* • Better selectivity and bioavailability *in vivo* • Modification of excretion route *in vivo*	• CDs quickly excreted from blood *in vivo* • Low complex stability (dynamic equilibrium) • The difficulties to control concentration -depended on CD effects in the target site *in vivo*
Micelles	
• Drug solubility • Lower dark phototoxicity *in vitro*	• Complicated uptake in tumor cells *in vitro* • Control release mechanisms are mandatory • Low penetration in tumor tissue *in vitro*
Solid polymer nanoparticles	
• Drug solubility • Lower dark phototoxicity *in vitro* • Better selectivity *in vivo* • Better PDT *in vivo*	• Complicated uptake in tumor cells *in vitro*
Silica-based NPs	
• Drug solubility • Better selectivity *in vivo* • Better PDT *in vivo* • Penetration through the blood-brain barrier *in vivo*	• Complicated uptake in tumor cells *in vitro* • Control release mechanisms are essential
Protein-based nanoparticles	
• Drug solubility	• No improvement of mTHPC accumulation and/or PDT efficiency

Liposomes	
• Drug solubility • Lower dark phototoxicity *in vitro* • Higher drug bioavailability *in vivo* • Better selectivity *in vivo* • Better PDT in short DLI *in vivo* • High vascular PDT damage • Possibility to encapsulate NPs	• Low penetration in tumor tissue *in vitro* • Complicated uptake in tumor cells *in vitro* • Low stability in blood *in vivo* • Quick release of drug *in vivo*
Extracellular vesicles	
• Drug solubility • Lower dark phototoxicity *in vitro* • Higher accumulation in tumor cells *in vitro* • Stability in serum *in vitro* • Improved penetration in tumor tissue *in vitro* • Better PDT in cells and spheroids *in vitro*	• Low efficiency of passive loading
Solid Lipid Nanoparticles	
• Drug solubility • Lower dark phototoxicity *in vitro* • Stability in serum *in vitro* • Higher drug bioavailability *in vivo*	• Complicated uptake in tumor cells *in vitro*
Carbon nanotubes	
• Drug solubility • Combination of PTT/PDT available	• Complicated uptake in tumor cells *in vitro*

Acknowledgments

This work was supported by the French “Ligue Nationale contre le Cancer (CCIR-GE)”, the Institut de Cancérologie de Lorraine, Belarusian Republican Foundation for Fundamental Research (BRFFR) [grant number M18MB-002] and the Ministry of Education of the Republc of Beloarus.

Disclosures

The authors report no declarations of interest

5. References

[1] S. Kwiatkowski, B. Knap, D. Przystupski, J. Saczko, E. Kędzierska, K. Knap-Czop, J. Kotlińska, O. Michel, K. Kotowski, J. Kulbacka, Photodynamic therapy - mechanisms, photosensitizers and combinations, Biomed. Pharmacother. Biomedecine Pharmacother. 106 (2018) 1098–1107. doi:10.1016/j.biopha.2018.07.049.

[2] D. van Straten, V. Mashayekhi, H.S. de Bruijn, S. Oliveira, D.J. Robinson, Oncologic Photodynamic Therapy: Basic Principles, Current Clinical Status and Future Directions, Cancers. 9 (2017). doi:10.3390/cancers9020019.

[3] D. Luo, K.A. Carter, D. Miranda, J.F. Lovell, Chemophototherapy: An Emerging Treatment Option for Solid Tumors, Adv. Sci. Weinh. Baden-Wurtt. Ger. 4 (2017) 1600106. doi:10.1002/advs.201600106.

[4] A.P. Castano, T.N. Demidova, M.R. Hamblin, Mechanisms in photodynamic therapy: Part three-Photosensitizer pharmacokinetics, biodistribution, tumor localization and modes of tumor destruction, Photodiagnosis Photodyn. Ther. 2 (2005) 91–106. doi:10.1016/S1572-1000(05)00060-8.

[5] J. Moan, K. Berg, The photodegradation of porphyrins in cells can be used to estimate the lifetime of singlet oxygen, Photochem. Photobiol. 53 (1991) 549–553.

[6] R.R. Allison, K. Moghissi, Photodynamic Therapy (PDT): PDT Mechanisms, Clin. Endosc. 46 (2013) 24–29. doi:10.5946/ce.2013.46.1.24.

[7] M.O. Senge, J.C. Brandt, Temoporfin (Foscan®, 5,10,15,20-tetra(m-hydroxyphenyl)chlorin)--a second-generation photosensitizer, Photochem. Photobiol. 87 (2011) 1240–1296. doi:10.1111/j.1751-1097.2011.00986.x.

[8] A.E. O'Connor, W.M. Gallagher, A.T. Byrne, Porphyrin and Nonporphyrin Photosensitizers in Oncology: Preclinical and Clinical Advances in Photodynamic Therapy, Photochem. Photobiol. 85 (2009) 1053–1074. doi:10.1111/j.1751-1097.2009.00585.x.

[9] EMA, Foscan, Eur. Med. Agency. (2018). https://www.ema.europa.eu/en/medicines/human/EPAR/foscan (accessed May 20, 2019).

[10] J.F. Savary, P. Grosjean, P. Monnier, C. Fontolliet, G. Wagnieres, D. Braichotte, H. van den Bergh, Photodynamic therapy of early squamous cell carcinomas of the esophagus: a review of 31 cases, Endoscopy. 30 (1998) 258–265. doi:10.1055/s-2007-1001252.

[11] J.F. Savary, P. Monnier, C. Fontolliet, J. Mizeret, G. Wagnières, D. Braichotte, H. van den Bergh, Photodynamic therapy for early squamous cell carcinomas of the esophagus, bronchi, and mouth with m-tetra (hydroxyphenyl) chlorin, Arch. Otolaryngol. Head Neck Surg. 123 (1997) 162–168.

[12] D.J. Ball, D.I. Vernon, S.B. Brown, The high photoactivity of m-THPC in photodynamic therapy. Unusually strong retention of m-THPC by RIF-1 cells in culture, Photochem. Photobiol. 69 (1999) 360–363. doi:10.1111/j.1751-1097.1999.tb03299.x.

[13] R. Bonnett, R.D. White, U.J. Winfield, M.C. Berenbaum, Hydroporphyrins of the meso-tetra(hydroxyphenyl)porphyrin series as tumour photosensitizers, Biochem. J. 261 (1989) 277–280.

[14] R. Bonnett, P. Charlesworth, B.D. Djelal, S. Foley, D.J. McGarvey, T.G. Truscott, Photophysical properties of 5,10,15,20-tetrakis(m-hydroxyphenyl)porphyrin (m-THPP), 5,10,15,20-tetrakis(m-hydroxyphenyl)chlorin (m-THPC) and 5,10,15,20-tetrakis(m-hydroxyphenyl)bacteriochlorin (m-THPBC): a comparative study, J. Chem. Soc. Perkin Trans. 2. (1999) 325–328. doi:10.1039/A805328F.

[15] N.V. Koudinova, J.H. Pinthus, A. Brandis, O. Brenner, P. Bendel, J. Ramon, Z. Eshhar, A. Scherz, Y. Salomon, Photodynamic therapy with Pd-bacteriopheophorbide (TOOKAD):

Successful in vivo treatment of human prostatic small cell carcinoma xenografts, Int. J. Cancer. 104 (2003) 782–789. doi:10.1002/ijc.11002.

[16] B.W. Pogue, R.W. Redmond, N. Trivedi, T. Hasan, Photophysical Properties of Tin Ethyl Etiopurpurin I (SnET2) and Tin Octaethylbenzochlorin (SnOEBC) in Solution and Bound to Albumin, Photochem. Photobiol. 68 (1998) 809–815. doi:10.1111/j.1751-1097.1998.tb05288.x.

[17] S. Mitra, T.H. Foster, Photophysical Parameters, Photosensitizer Retention and Tissue Optical Properties Completely Account for the Higher Photodynamic Efficacy of meso-Tetra-Hydroxyphenyl-Chlorin vs Photofrin¶, Photochem. Photobiol. 81 (2005) 849–859. doi:10.1111/j.1751-1097.2005.tb01453.x.

[18] I. Laville, T. Figueiredo, B. Loock, S. Pigaglio, P. Maillard, D.S. Grierson, D. Carrez, A. Croisy, J. Blais, Synthesis, cellular internalization and photodynamic activity of glucoconjugated derivatives of tri and tetra(meta-hydroxyphenyl)chlorins, Bioorg. Med. Chem. 11 (2003) 1643–1652.

[19] M.O. Senge, J.C. Brandt, Temoporfin (Foscan®, 5,10,15,20-tetra(m-hydroxyphenyl)chlorin)--a second-generation photosensitizer, Photochem. Photobiol. 87 (2011) 1240–1296. doi:10.1111/j.1751-1097.2011.00986.x.

[20] J.Y. Chen, N.K. Mak, C.M.N. Yow, M.C. Fung, L.C. Chiu, W.N. Leung, N.H. Cheung, The Binding Characteristics and Intracellular Localization of Temoporfin (mTHPC) in Myeloid Leukemia Cells: Phototoxicity and Mitochondrial Damage¶, Photochem. Photobiol. 72 (2000) 541–547. doi:10.1562/0031-8655(2000)0720541TBCAIL2.0.CO2.

[21] S. Sasnouski, V. Zorin, I. Khludeyev, M.-A. D'Hallewin, F. Guillemin, L. Bezdetnaya, Investigation of Foscan interactions with plasma proteins, Biochim. Biophys. Acta. 1725 (2005) 394–402. doi:10.1016/j.bbagen.2005.06.014.

[22] V.O. Melnikova, L.N. Bezdetnaya, C. Bour, E. Festor, M.P. Gramain, J.L. Merlin, null Potapenko AYa, F. Guillemin, Subcellular localization of meta-tetra (hydroxyphenyl) chlorin in human tumor cells subjected to photodynamic treatment, J. Photochem. Photobiol. B. 49 (1999) 96–103.

[23] M. Triesscheijn, M. Ruevekamp, R. Out, T.J.C. Van Berkel, J. Schellens, P. Baas, F.A. Stewart, The pharmacokinetic behavior of the photosensitizer meso-tetra-hydroxyphenyl-chlorin in mice and men, Cancer Chemother. Pharmacol. 60 (2007) 113–122. doi:10.1007/s00280-006-0356-9.

[24] T. Kiesslich, J. Berlanda, K. Plaetzer, B. Krammer, F. Berr, Comparative characterization of the efficiency and cellular pharmacokinetics of Foscan- and Foslip-based photodynamic treatment in human biliary tract cancer cell lines, Photochem. Photobiol. Sci. Off. J. Eur. Photochem. Assoc. Eur. Soc. Photobiol. 6 (2007) 619–627. doi:10.1039/b617659c.

[25] I. Opitz, T. Krueger, Y. Pan, H.-J. Altermatt, G. Wagnières, H.-B. Ris, Preclinical comparison of mTHPC and verteporfin for intracavitary photodynamic therapy of malignant pleural mesothelioma, Eur. Surg. Res. Eur. Chir. Forsch. Rech. Chir. Eur. 38 (2006) 333–339. doi:10.1159/000094028.

[26] S. Marchal, A. Fadloun, E. Maugain, M.-A. D'Hallewin, F. Guillemin, L. Bezdetnaya, Necrotic and apoptotic features of cell death in response to Foscan photosensitization of HT29 monolayer and multicell spheroids, Biochem. Pharmacol. 69 (2005) 1167–1176. doi:10.1016/j.bcp.2005.01.021.

[27] S. Mitra, E. Maugain, L. Bolotine, F. Guillemin, T.H. Foster, Temporally and spatially heterogeneous distribution of mTHPC in a murine tumor observed by two-color confocal fluorescence imaging and spectroscopy in a whole-mount model, Photochem. Photobiol. 81 (2005) 1123–1130. doi:10.1562/2005-03-24-RA-471.

[28] M.O. Senge, mTHPC – A drug on its way from second to third generation photosensitizer?, Photodiagnosis Photodyn. Ther. 9 (2012) 170–179. doi:10.1016/j.pdpdt.2011.10.001.
[29] R. Baskaran, J. Lee, S.-G. Yang, Clinical development of photodynamic agents and therapeutic applications, Biomater. Res. 22 (2018) 25. doi:10.1186/s40824-018-0140-z.
[30] P. Westermann, T. Gianzmann, S. Andrejevic, D.R. Braichotte, M. Forrer, G.A. Wagnieres, P. Monnier, H. Van Den Bergh, J.-P. Mach, S. Folli, Long circulating half-life and high tumor selectivity of the photosensitizer meta-tetrahydroxyphenylchlorin conjugated to polyethylene glycol in nude mice grafted with a human colon carcinoma, Int. J. Cancer. 76 (1998) 842–850. doi:10.1002/(SICI)1097-0215(19980610)76:6<842::AID-IJC13>3.0.CO;2-4.
[31] P. Westermann, T.M. Glanzmann, S. Folli, D. Braichotte, M. Forrer, S. Andrejevic-Blant, J.-P. Mach, P. Monnier, H. van den Bergh, Comparison of the influence of a water-soluble polymer carrier on the tumor localization and biodistribution of mesotetrametahydroxyphenylchlorin (mTHPC) in two animal models, in: 5th Int. Photodyn. Assoc. Bienn. Meet., International Society for Optics and Photonics, 1995: pp. 45–51. doi:10.1117/12.203361.
[32] M.F. Grahn, A. Giger, A. McGuinness, M.L. de Jode, J.C. Stewart, H.B. Ris, H.J. Altermatt, N.S. Williams, mTHPC Polymer Conjugates: The In Vivo Photodynamic Activity of Four Candidate Compounds, Lasers Med. Sci. 14 (1999) 40–46. doi:10.1007/s101030050019.
[33] M.F. Grahn, A. McGuinness, M.L. de Jode, A. Giger, A.S. Dhiman, C.-M. Cheung, S. Pavitt, R. Benzie, N.S. Williams, In-vivo photodynamic activity of mTHPC poly(ethylene glycol) conjugates (SC102), in: Photochem. Photodyn. Ther. Modalities III, International Society for Optics and Photonics, 1997: pp. 180–187. doi:10.1117/12.297801.
[34] H.B. Ris, Q. Li, T. Krueger, C.K. Lim, B. Reynolds, U. Althaus, H.J. Altermatt, Photosensitizing effects of m-tetrahydroxyphenylchlorin on human tumor xenografts: correlation with sensitizer uptake, tumor doubling time and tumor histology, Int. J. Cancer. 76 (1998) 872–874.
[35] T. Reuther, A.C. Kübler, U. Zillmann, C. Flechtenmacher, H. Sinn, Comparison of the in vivo efficiency of photofrin II-, mTHPC-, mTHPC-PEG- and mTHPCnPEG-mediated PDT in a human xenografted head and neck carcinoma, Lasers Surg. Med. 29 (2001) 314–322.
[36] J. Gravier, R. Schneider, C. Frochot, T. Bastogne, F. Schmitt, J. Didelon, F. Guillemin, M. Barberi-Heyob, Improvement of meta-tetra(hydroxyphenyl)chlorin-like photosensitizer selectivity with folate-based targeted delivery. synthesis and in vivo delivery studies, J. Med. Chem. 51 (2008) 3867–3877. doi:10.1021/jm800125a.
[37] M.B. Vrouenraets, G.W.M. Visser, M. Stigter, H. Oppelaar, G.B. Snow, G.A.M.S. van Dongen, Comparison of aluminium (III) phthalocyanine tetrasulfonate- and meta-tetrahydroxyphenylchlorin-monoclonal antibody conjugates for their efficacy in photodynamic therapy in vitro, Int. J. Cancer. 98 (2002) 793–798.
[38] M.B. Vrouenraets, G.W.M. Visser, F.A. Stewart, M. Stigter, H. Oppelaar, P.E. Postmus, G.B. Snow, G.A.M.S. van Dongen, Development of meta-Tetrahydroxyphenylchlorin-Monoclonal Antibody Conjugates for Photoimmunotherapy, Cancer Res. 59 (1999) 1505–1513.
[39] L. Rogers, N.N. Sergeeva, E. Paszko, G.M.F. Vaz, M.O. Senge, Lead Structures for Applications in Photodynamic Therapy. 6. Temoporfin Anti-Inflammatory Conjugates to Target the Tumor Microenvironment for In Vitro PDT, PloS One. 10 (2015) e0125372. doi:10.1371/journal.pone.0125372.
[40] E. Haimov, H. Weitman, S. Polani, H. Schori, D. Zitoun, O. Shefi, meso-Tetrahydroxyphenylchlorin-Conjugated Gold Nanoparticles as a Tool To Improve Photodynamic Therapy, ACS Appl. Mater. Interfaces. 10 (2018) 2319–2327. doi:10.1021/acsami.7b16455.

[41] I. Yakavets, I. Yankovsky, M. Millard, L. Lamy, H.-P. Lassalle, A. Wiehe, V. Zorin, L. Bezdetnaya, The alteration of temoporfin distribution in multicellular tumor spheroids by β-cyclodextrins, Int. J. Pharm. 529 (2017) 568–575. doi:10.1016/j.ijpharm.2017.07.037.
[42] I. Yankovsky, E. Bastien, I. Yakavets, I. Khludeyev, H.-P. Lassalle, S. Gräfe, L. Bezdetnaya, V. Zorin, Inclusion complexation with β-cyclodextrin derivatives alters photodynamic activity and biodistribution of meta-tetra(hydroxyphenyl)chlorin, Eur. J. Pharm. Sci. Off. J. Eur. Fed. Pharm. Sci. 91 (2016) 172–182. doi:10.1016/j.ejps.2016.06.012.
[43] J.-W. Hofman, M.G. Carstens, F. van Zeeland, C. Helwig, F.M. Flesch, W.E. Hennink, C.F. van Nostrum, Photocytotoxicity of mTHPC (Temoporfin) Loaded Polymeric Micelles Mediated by Lipase Catalyzed Degradation, Pharm. Res. 25 (2008) 2065–2073. doi:10.1007/s11095-008-9590-7.
[44] O. Bourdon, V. Mosqueira, P. Legrand, J. Blais, A comparative study of the cellular uptake, localization and phototoxicity of meta-tetra(hydroxyphenyl) chlorin encapsulated in surface-modified submicronic oil/water carriers in HT29 tumor cells, J. Photochem. Photobiol. B. 55 (2000) 164–171. doi:10.1016/S1011-1344(00)00043-9.
[45] M.-J. Shieh, C.-L. Peng, W.-L. Chiang, C.-H. Wang, C.-Y. Hsu, S.-J.J. Wang, P.-S. Lai, Reduced skin photosensitivity with meta-tetra(hydroxyphenyl)chlorin-loaded micelles based on a poly(2-ethyl-2-oxazoline)-b-poly(d,l-lactide) diblock copolymer in vivo, Mol. Pharm. 7 (2010) 1244–1253. doi:10.1021/mp100060v.
[46] C.-L. Peng, L.-Y. Yang, T.-Y. Luo, P.-S. Lai, S.-J. Yang, W.-J. Lin, M.-J. Shieh, Development of pH sensitive 2-(diisopropylamino)ethyl methacrylate based nanoparticles for photodynamic therapy, Nanotechnology. 21 (2010) 155103. doi:10.1088/0957-4484/21/15/155103.
[47] J. Wu, S. Feng, W. Liu, F. Gao, Y. Chen, Targeting integrin-rich tumors with temoporfin-loaded vitamin-E-succinate-grafted chitosan oligosaccharide/d-α-tocopheryl polyethylene glycol 1000 succinate nanoparticles to enhance photodynamic therapy efficiency, Int. J. Pharm. 528 (2017) 287–298. doi:10.1016/j.ijpharm.2017.06.021.
[48] Y. Liu, J.-W. de Vries, Q. Liu, A. Hartman, G. Wieland, S. Wieczorek, H. Boerner, A. Wiehe, E. Buhler, M. Stuart, W. Browne, A. Herrmann, A.K.H. Hirsch, Lipid-DNAs as Solubilizers of mTHPC, Chem. - Eur. J. (2017). doi:10.1002/chem.201705206.
[49] J.W.H. Wennink, Y. Liu, P.I. Mäkinen, F. Setaro, A. de la Escosura, M. Bourajjaj, J.P. Lappalainen, L.P. Holappa, J.B. van den Dikkenberg, M. al Fartousi, P.N. Trohopoulos, S. Ylä-Herttuala, T. Torres, W.E. Hennink, C.F. van Nostrum, Macrophage selective photodynamic therapy by meta-tetra(hydroxyphenyl)chlorin loaded polymeric micelles: A possible treatment for cardiovascular diseases, Eur. J. Pharm. Sci. 107 (2017) 112–125. doi:10.1016/j.ejps.2017.06.038.
[50] Gao De, Xu Hao, Philbert Martin A., Kopelman Raoul, Ultrafine Hydrogel Nanoparticles: Synthetic Approach and Therapeutic Application in Living Cells, Angew. Chem. Int. Ed. 46 (2007) 2224–2227. doi:10.1002/anie.200603927.
[51] K. Löw, T. Knobloch, S. Wagner, A. Wiehe, A. Engel, K. Langer, H. von Briesen, Comparison of intracellular accumulation and cytotoxicity of free mTHPC and mTHPC-loaded PLGA nanoparticles in human colon carcinoma cells, Nanotechnology. 22 (2011) 245102. doi:10.1088/0957-4484/22/24/245102.
[52] M. Rojnik, P. Kocbek, F. Moret, C. Compagnin, L. Celotti, M.J. Bovis, J.H. Woodhams, A.J. Macrobert, D. Scheglmann, W. Helfrich, M.J. Verkaik, E. Papini, E. Reddi, J. Kos, In vitro and in vivo characterization of temoporfin-loaded PEGylated PLGA nanoparticles for use in photodynamic therapy, Nanomed. 7 (2012) 663–677. doi:10.2217/nnm.11.130.

[53] M. Villa Nova, C. Janas, M. Schmidt, T. Ulshoefer, S. Gräfe, S. Schiffmann, N. de Bruin, A. Wiehe, V. Albrecht, M.J. Parnham, M. Luciano Bruschi, M.G. Wacker, Nanocarriers for photodynamic therapy—rational formulation design and medium-scale manufacture, Int. J. Pharm. 491 (2015) 250–260. doi:10.1016/j.ijpharm.2015.06.024.
[54] C. Compagnin, L. Baù, M. Mognato, L. Celotti, G. Miotto, M. Arduini, F. Moret, C. Fede, F. Selvestrel, I.M.R. Echevarria, F. Mancin, E. Reddi, The cellular uptake of meta-tetra(hydroxyphenyl)chlorin entrapped in organically modified silica nanoparticles is mediated by serum proteins, Nanotechnology. 20 (2009) 345101. doi:10.1088/0957-4484/20/34/345101.
[55] K. Haedicke, D. Kozlova, S. Gräfe, U. Teichgräber, M. Epple, I. Hilger, Multifunctional calcium phosphate nanoparticles for combining near-infrared fluorescence imaging and photodynamic therapy, Acta Biomater. 14 (2015) 197–207. doi:10.1016/j.actbio.2014.12.009.
[56] I. Brezániová, K. Záruba, J. Králová, A. Sinica, H. Adámková, P. Ulbrich, P. Poučková, M. Hrubý, P. Štěpánek, V. Král, Silica-based nanoparticles are efficient delivery systems for temoporfin, Photodiagnosis Photodyn. Ther. 21 (2018) 275–284. doi:10.1016/j.pdpdt.2017.12.014.
[57] K. Chen, M. Wacker, S. Hackbarth, C. Ludwig, K. Langer, B. Röder, Photophysical evaluation of mTHPC-loaded HSA nanoparticles as novel PDT delivery systems, J. Photochem. Photobiol. B. 101 (2010) 340–347. doi:10.1016/j.jphotobiol.2010.08.006.
[58] A. Preuß, K. Chen, S. Hackbarth, M. Wacker, K. Langer, B. Röder, Photosensitizer loaded HSA nanoparticles II: In vitro investigations, Int. J. Pharm. 404 (2011) 308–316. doi:10.1016/j.ijpharm.2010.11.023.
[59] B. Pegaz, E. Debefve, J.-P. Ballini, G. Wagnières, S. Spaniol, V. Albrecht, D.V. Scheglmann, N.E. Nifantiev, H. van den Bergh, Y.N. Konan-Kouakou, Photothrombic activity of m-THPC-loaded liposomal formulations: Pre-clinical assessment on chick chorioallantoic membrane model, Eur. J. Pharm. Sci. 28 (2006) 134–140. doi:10.1016/j.ejps.2006.01.008.
[60] A. Johansson, J. Svensson, N. Bendsoe, K. Svanberg, E. Alexandratou, M. Kyriazi, D. Yova, S. Gräfe, T. Trebst, S. Andersson-Engels, Fluorescence and absorption assessment of a lipid mTHPC formulation following topical application in a non-melanotic skin tumor model, J. Biomed. Opt. 12 (2007) 034026. doi:10.1117/1.2743080.
[61] J. Svensson, A. Johansson, S. Gräfe, B. Gitter, T. Trebst, N. Bendsoe, S. Andersson-Engels, K. Svanberg, Tumor selectivity at short times following systemic administration of a liposomal temoporfin formulation in a murine tumor model, Photochem. Photobiol. 83 (2007) 1211–1219. doi:10.1111/j.1751-1097.2007.00146.x.
[62] M.A. D'Hallewin, D. Kochetkov, Y. Viry-Babel, A. Leroux, E. Werkmeister, D. Dumas, S. Gräfe, V. Zorin, F. Guillemin, L. Bezdetnaya, Photodynamic therapy with intratumoral administration of Lipid-Based mTHPC in a model of breast cancer recurrence, Lasers Surg. Med. 40 (2008) 543–549. doi:10.1002/lsm.20662.
[63] H.-P. Lassalle, M. Wagner, L. Bezdetnaya, F. Guillemin, H. Schneckenburger, Fluorescence imaging of Foscan® and Foslip in the plasma membrane and in whole cells, J. Photochem. Photobiol. B. 92 (2008) 47–53. doi:10.1016/j.jphotobiol.2008.04.007.
[64] H.-P. Lassalle, D. Dumas, S. Gräfe, M.-A. D'Hallewin, F. Guillemin, L. Bezdetnaya, Correlation between in vivo pharmacokinetics, intratumoral distribution and photodynamic efficiency of liposomal mTHPC, J. Control. Release Off. J. Control. Release Soc. 134 (2009) 118–124. doi:10.1016/j.jconrel.2008.11.016.
[65] J. Garrier, L. Bezdetnaya, C. Barlier, S. Gräfe, F. Guillemin, M.-A. D'Hallewin, Foslip®-based photodynamic therapy as a means to improve wound healing, Photodiagnosis Photodyn. Ther. 8 (2011) 321–327. doi:10.1016/j.pdpdt.2011.06.003.

[66] E.B. Gyenge, S. Hiestand, S. Graefe, H. Walt, C. Maake, Cellular and molecular effects of the liposomal mTHPC derivative Foslipos in prostate carcinoma cells in vitro, Photodiagnosis Photodyn. Ther. 8 (2011) 86–96. doi:10.1016/j.pdpdt.2011.02.001.
[67] S.A.H.J. de Visscher, S. Kaščáková, H.S. de Bruijn, A. van der P.- van den Heuvel, A. Amelink, H.J.C.M. Sterenborg, D.J. Robinson, J.L.N. Roodenburg, M.J.H. Witjes, Fluorescence localization and kinetics of mTHPC and liposomal formulations of mTHPC in the window-chamber tumor model, Lasers Surg. Med. 43 (2011) 528–536. doi:10.1002/lsm.21082.
[68] S.A.H.J. de Visscher, M.J.H. Witjes, B. van der Vegt, H.S. de Bruijn, A. van der Ploeg - van den Heuvel, A. Amelink, H.J.C.M. Sterenborg, J.L.N. Roodenburg, D.J. Robinson, Localization of liposomal mTHPC formulations within normal epithelium, dysplastic tissue, and carcinoma of oral epithelium in the 4NQO-carcinogenesis rat model: LOCALIZATION OF LIPOSOMAL mTHPC FORMULATIONS, Lasers Surg. Med. 45 (2013) 668–678. doi:10.1002/lsm.22197.
[69] J. Garrier, V. Reshetov, S. Gräfe, F. Guillemin, V. Zorin, L. Bezdetnaya, Factors affecting the selectivity of nanoparticle-based photoinduced damage in free and xenografted chorioallantoïc membrane model, J. Drug Target. (2013). doi:10.3109/1061186X.2013.860981.
[70] V. Reshetov, H.-P. Lassalle, A. François, D. Dumas, S. Hupont, S. Gräfe, V. Filipe, W. Jiskoot, F. Guillemin, V. Zorin, L. Bezdetnaya, Photodynamic therapy with conventional and PEGylated liposomal formulations of mTHPC (temoporfin): comparison of treatment efficacy and distribution characteristics in vivo, Int. J. Nanomedicine. 8 (2013) 3817–3831. doi:10.2147/IJN.S51002.
[71] K. Haedicke, S. Gräfe, F. Lehmann, I. Hilger, Multiplexed in vivo fluorescence optical imaging of the therapeutic efficacy of photodynamic therapy, Biomaterials. 34 (2013) 10075–10083. doi:10.1016/j.biomaterials.2013.08.087.
[72] A. Reinhard, A. Bressenot, R. Dassonneville, A. Loywick, D. Hot, C. Audebert, S. Marchal, F. Guillemin, M. Chamaillard, L. Peyrin-Biroulet, L. Bezdetnaya, Photodynamic therapy relieves colitis and prevents colitis-associated carcinogenesis in mice, Inflamm. Bowel Dis. 21 (2015) 985–995. doi:10.1097/MIB.0000000000000354.
[73] E. Gaio, D. Scheglmann, E. Reddi, F. Moret, Uptake and photo-toxicity of Foscan®, Foslip® and Fospeg® in multicellular tumor spheroids, J. Photochem. Photobiol. B. 161 (2016) 244–252. doi:10.1016/j.jphotobiol.2016.05.011.
[74] D. Hinger, S. Gräfe, F. Navarro, B. Spingler, D. Pandiarajan, H. Walt, A.-C. Couffin, C. Maake, Lipid nanoemulsions and liposomes improve photodynamic treatment efficacy and tolerance in CAL-33 tumor bearing nude mice, J. Nanobiotechnology. 14 (2016) 71. doi:10.1186/s12951-016-0223-8.
[75] D. Meier, S.M. Botter, C. Campanile, B. Robl, S. Gräfe, G. Pellegrini, W. Born, B. Fuchs, Foscan and foslip based photodynamic therapy in osteosarcoma in vitro and in intratibial mouse models, Int. J. Cancer. 140 (2017) 1680–1692. doi:10.1002/ijc.30572.
[76] I. Yakavets, H.-P. Lassalle, D. Scheglmann, A. Wiehe, V. Zorin, L. Bezdetnaya, I. Yakavets, H.-P. Lassalle, D. Scheglmann, A. Wiehe, V. Zorin, L. Bezdetnaya, Temoporfin-in-Cyclodextrin-in-Liposome—A New Approach for Anticancer Drug Delivery: The Optimization of Composition, Nanomaterials. 8 (2018) 847. doi:10.3390/nano8100847.
[77] M. Millard, I. Yakavets, M. Piffoux, A. Brun, F. Gazeau, J.-M. Guigner, J. Jasniewski, H.-P. Lassalle, C. Wilhelm, L. Bezdetnaya, mTHPC-loaded extracellular vesicles outperform liposomal and free mTHPC formulations by an increased stability, drug delivery efficiency

and cytotoxic effect in tridimensional model of tumors, Drug Deliv. 25 (2018) 1790–1801. doi:10.1080/10717544.2018.1513609.
[78] J. Buchholz, B. Kaser-Hotz, T. Khan, C. Rohrer Bley, K. Melzer, R.A. Schwendener, M. Roos, H. Walt, Optimizing photodynamic therapy: in vivo pharmacokinetics of liposomal meta-(tetrahydroxyphenyl)chlorin in feline squamous cell carcinoma, Clin. Cancer Res. Off. J. Am. Assoc. Cancer Res. 11 (2005) 7538–7544. doi:10.1158/1078-0432.CCR-05-0490.
[79] J. Berlanda, T. Kiesslich, V. Engelhardt, B. Krammer, K. Plaetzer, Comparative in vitro study on the characteristics of different photosensitizers employed in PDT, J. Photochem. Photobiol. B. 100 (2010) 173–180. doi:10.1016/j.jphotobiol.2010.06.004.
[80] C. Compagnin, F. Moret, L. Celotti, G. Miotto, J.H. Woodhams, A.J. MacRobert, D. Scheglmann, S. Iratni, E. Reddi, Meta-tetra(hydroxyphenyl)chlorin-loaded liposomes sterically stabilised with poly(ethylene glycol) of different length and density: characterisation, in vitro cellular uptake and phototoxicity, Photochem. Photobiol. Sci. Off. J. Eur. Photochem. Assoc. Eur. Soc. Photobiol. 10 (2011) 1751–1759. doi:10.1039/c1pp05163f.
[81] M.J. Bovis, J.H. Woodhams, M. Loizidou, D. Scheglmann, S.G. Bown, A.J. Macrobert, Improved in vivo delivery of m-THPC via pegylated liposomes for use in photodynamic therapy, J. Control. Release Off. J. Control. Release Soc. 157 (2012) 196–205. doi:10.1016/j.jconrel.2011.09.085.
[82] A. Petri, D. Yova, E. Alexandratou, M. Kyriazi, M. Rallis, Comparative characterization of the cellular uptake and photodynamic efficiency of Foscan® and Fospeg in a human prostate cancer cell line, Photodiagnosis Photodyn. Ther. 9 (2012) 344–354. doi:10.1016/j.pdpdt.2012.03.008.
[83] H. Xie, P. Svenmarker, J. Axelsson, S. Gräfe, M. Kyriazi, N. Bendsoe, S. Andersson-Engels, K. Svanberg, Pharmacokinetic and biodistribution study following systemic administration of Fospeg® - a Pegylated liposomal mTHPC formulation in a murine model: Pharmacokinetic and biodistribution study following systemic administration of Fospeg®, J. Biophotonics. 8 (2015) 142–152. doi:10.1002/jbio.201300133.
[84] R.W.K. Wu, E.S.M. Chu, Z. Huang, C.S. Xu, C.W. Ip, C.M.N. Yow, Effect of FosPeg® mediated photoactivation on P-gp/ABCB1 protein expression in human nasopharyngeal carcinoma cells, J. Photochem. Photobiol. B. 148 (2015) 82–87. doi:10.1016/j.jphotobiol.2015.03.019.
[85] C. Bombelli, A. Stringaro, S. Borocci, G. Bozzuto, M. Colone, L. Giansanti, R. Sgambato, L. Toccaceli, G. Mancini, A. Molinari, Efficiency of liposomes in the delivery of a photosensitizer controlled by the stereochemistry of a gemini surfactant component, Mol. Pharm. 7 (2010) 130–137. doi:10.1021/mp900173v.
[86] C. Bombelli, G. Caracciolo, P. Di Profio, M. Diociaiuti, P. Luciani, G. Mancini, C. Mazzuca, M. Marra, A. Molinari, D. Monti, L. Toccacieli, M. Venanzi, Inclusion of a Photosensitizer in Liposomes Formed by DMPC/Gemini Surfactant: Correlation between Physicochemical and Biological Features of the Complexes, J. Med. Chem. 48 (2005) 4882–4891. doi:10.1021/jm050182d.
[87] A. Molinari, C. Bombelli, S. Mannino, A. Stringaro, L. Toccacieli, A. Calcabrini, M. Colone, A. Mangiola, G. Maira, P. Luciani, G. Mancini, G. Arancia, m-THPC-mediated photodynamic therapy of malignant gliomas: assessment of a new transfection strategy, Int. J. Cancer. 121 (2007) 1149–1155. doi:10.1002/ijc.22793.
[88] A. Molinari, M. Colone, A. Calcabrini, A. Stringaro, L. Toccacieli, G. Arancia, S. Mannino, A. Mangiola, G. Maira, C. Bombelli, G. Mancini, Cationic liposomes, loaded with m-THPC, in photodynamic therapy for malignant glioma, Toxicol. In Vitro. 21 (2007) 230–234. doi:10.1016/j.tiv.2006.09.006.

[89] N. Dragicevic-Curic, S. Gräfe, V. Albrecht, A. Fahr, Topical application of temoporfin-loaded invasomes for photodynamic therapy of subcutaneously implanted tumours in mice: A pilot study, J. Photochem. Photobiol. B. 91 (2008) 41–50. doi:10.1016/j.jphotobiol.2008.01.009.
[90] N. Dragicevic-Curic, D. Scheglmann, V. Albrecht, A. Fahr, Development of different temoporfin-loaded invasomes—novel nanocarriers of temoporfin: Characterization, stability and in vitro skin penetration studies, Colloids Surf. B Biointerfaces. 70 (2009) 198–206. doi:10.1016/j.colsurfb.2008.12.030.
[91] N. Dragicevic-Curic, S. Gräfe, B. Gitter, S. Winter, A. Fahr, Surface charged temoporfin-loaded flexible vesicles: In vitro skin penetration studies and stability, Int. J. Pharm. 384 (2010) 100–108. doi:10.1016/j.ijpharm.2009.10.006.
[92] M. Piffoux, A.K.A. Silva, C. Wilhelm, F. Gazeau, D. Tareste, Modification of Extracellular Vesicles by Fusion with Liposomes for the Design of Personalized Biogenic Drug Delivery Systems, ACS Nano. 12 (2018) 6830–6842. doi:10.1021/acsnano.8b02053.
[93] F.P. Navarro, G. Creusat, C. Frochot, A. Moussaron, M. Verhille, R. Vanderesse, J.-S. Thomann, P. Boisseau, I. Texier, A.-C. Couffin, M. Barberi-Heyob, Preparation and characterization of mTHPC-loaded solid lipid nanoparticles for photodynamic therapy, J. Photochem. Photobiol. B. 130 (2014) 161–169. doi:10.1016/j.jphotobiol.2013.11.007.
[94] D. Hinger, F. Navarro, A. Käch, J.-S. Thomann, F. Mittler, A.-C. Couffin, C. Maake, Photoinduced effects of m-tetrahydroxyphenylchlorin loaded lipid nanoemulsions on multicellular tumor spheroids, J. Nanobiotechnology. 14 (2016). doi:10.1186/s12951-016-0221-x.
[95] I. Brezaniova, M. Hruby, J. Kralova, V. Kral, Z. Cernochova, P. Cernoch, M. Slouf, J. Kredatusova, P. Stepanek, Temoporfin-loaded 1-tetradecanol-based thermoresponsive solid lipid nanoparticles for photodynamic therapy, J. Controlled Release. 241 (2016) 34–44. doi:10.1016/j.jconrel.2016.09.009.
[96] I. Marangon, C. Ménard-Moyon, A.K.A. Silva, A. Bianco, N. Luciani, F. Gazeau, Synergic mechanisms of photothermal and photodynamic therapies mediated by photosensitizer/carbon nanotube complexes, Carbon. 97 (2016) 110–123. doi:10.1016/j.carbon.2015.08.023.
[97] A.K.A. Silva, N. Luciani, F. Gazeau, K. Aubertin, S. Bonneau, C. Chauvierre, D. Letourneur, C. Wilhelm, Combining magnetic nanoparticles with cell derived microvesicles for drug loading and targeting, Nanomedicine Nanotechnol. Biol. Med. 11 (2015) 645–655. doi:10.1016/j.nano.2014.11.009.
[98] A.K.A. Silva, J. Kolosnjaj-Tabi, S. Bonneau, I. Marangon, N. Boggetto, K. Aubertin, O. Clément, M.F. Bureau, N. Luciani, F. Gazeau, C. Wilhelm, Magnetic and Photoresponsive Theranosomes: Translating Cell-Released Vesicles into Smart Nanovectors for Cancer Therapy, ACS Nano. 7 (2013) 4954–4966. doi:10.1021/nn400269x.
[99] R. Di Corato, G. Béalle, J. Kolosnjaj-Tabi, A. Espinosa, O. Clément, A.K.A. Silva, C. Ménager, C. Wilhelm, Combining Magnetic Hyperthermia and Photodynamic Therapy for Tumor Ablation with Photoresponsive Magnetic Liposomes, ACS Nano. 9 (2015) 2904–2916. doi:10.1021/nn506949t.
[100] Y.-C. Tsai, P. Vijayaraghavan, W.-H. Chiang, H.-H. Chen, T.-I. Liu, M.-Y. Shen, A. Omoto, M. Kamimura, K. Soga, H.-C. Chiu, Targeted Delivery of Functionalized Upconversion Nanoparticles for Externally Triggered Photothermal/Photodynamic Therapies of Brain Glioblastoma, Theranostics. 8 (2018) 1435–1448. doi:10.7150/thno.22482.
[101] A. Bautista-Sanchez, A. Kasselouri, M.-C. Desroches, J. Blais, P. Maillard, D.M. de Oliveira, A.C. Tedesco, P. Prognon, J. Delaire, Photophysical properties of glucoconjugated chlorins

and porphyrins and their associations with cyclodextrins, J. Photochem. Photobiol. B. 81 (2005) 154–162. doi:10.1016/j.jphotobiol.2005.05.013.
[102] H.-J. Sinn, H.-H. Schrenk, W. Maier-Borst, E. Friedrich, G. Graschew, D. WÖHRLE, T. Klenner, Polyethersubstituierte tumormittel, WO1991018630A1, 1991. https://patents.google.com/patent/WO1991018630A1/en?oq=WO+91%2f18630 (accessed March 17, 2019).
[103] J.K. Armstrong, R.B. Wenby, H.J. Meiselman, T.C. Fisher, The Hydrodynamic Radii of Macromolecules and Their Effect on Red Blood Cell Aggregation, Biophys. J. 87 (2004) 4259–4270. doi:10.1529/biophysj.104.047746.
[104] L.W. Seymour, Passive tumor targeting of soluble macromolecules and drug conjugates, Crit. Rev. Ther. Drug Carrier Syst. 9 (1992) 135–187.
[105] S.G. Schultz, A.K. Solomon, Determination of the Effective Hydrodynamic Radii of Small Molecules by Viscometry, J. Gen. Physiol. 44 (1961) 1189–1199. doi:10.1085/jgp.44.6.1189.
[106] R.B. Hamanaka, N.S. Chandel, Targeting glucose metabolism for cancer therapy, J. Exp. Med. 209 (2012) 211–215. doi:10.1084/jem.20120162.
[107] A. Cheung, H.J. Bax, D.H. Josephs, K.M. Ilieva, G. Pellizzari, J. Opzoomer, J. Bloomfield, M. Fittall, A. Grigoriadis, M. Figini, S. Canevari, J.F. Spicer, A.N. Tutt, S.N. Karagiannis, Targeting folate receptor alpha for cancer treatment, Oncotarget. 7 (2016) 52553–52574. doi:10.18632/oncotarget.9651.
[108] S. Jain, D.G. Hirst, J.M. O'Sullivan, Gold nanoparticles as novel agents for cancer therapy, Br. J. Radiol. 85 (2012) 101–113. doi:10.1259/bjr/59448833.
[109] R. Meir, K. Shamalov, O. Betzer, M. Motiei, M. Horovitz-Fried, R. Yehuda, A. Popovtzer, R. Popovtzer, C.J. Cohen, Nanomedicine for Cancer Immunotherapy: Tracking Cancer-Specific T-Cells in Vivo with Gold Nanoparticles and CT Imaging, ACS Nano. 9 (2015) 6363–6372. doi:10.1021/acsnano.5b01939.
[110] F. Giuntini, C.M.A. Alonso, R.W. Boyle, Synthetic approaches for the conjugation of porphyrins and related macrocycles to peptides and proteins, Photochem. Photobiol. Sci. Off. J. Eur. Photochem. Assoc. Eur. Soc. Photobiol. 10 (2011) 759–791. doi:10.1039/c0pp00366b.
[111] A. Ben Mihoub, L. Larue, A. Moussaron, Z. Youssef, L. Colombeau, F. Baros, C. Frochot, R. Vanderesse, S. Acherar, Use of Cyclodextrins in Anticancer Photodynamic Therapy Treatment, Molecules. 23 (2018) 1936. doi:10.3390/molecules23081936.
[112] D. Demore, A. Kasselouri, O. Bourdon, J. Blais, G. Mahuzier, P. Prognon, Enhancement of 5,10,15,20-Tetra(m-Hydroxyphenyl)chlorin Fluorescence Emission by Inclusion in Natural and Modified Cyclodextrins, Appl. Spectrosc. 53 (1999) 523–527.
[113] I. Yakavets, I. Yankovsky, L. Bezdetnaya, V. Zorin, Soret band shape indicates mTHPC distribution between β-cyclodextrins and serum proteins, Dyes Pigments. 137 (2017) 299–306. doi:10.1016/j.dyepig.2016.11.007.
[114] M.-C. Desroches, A. Kasselouri, O. Bourdon, P. Chaminade, J. Blais, P. Prognon, A direct sensitized fluorimetric determination of5,10,15,20-tetra(m-hydroxyphenyl)chlorin [m-THPC(Foscan)®] in human plasma using a cyclodextrin inclusion complex, Analyst. 126 (2001) 923–927. doi:10.1039/B100808K.
[115] I. Yakavets, H.-P. Lassalle, I. Yankovsky, F. Ingrosso, A. Monari, L. Bezdetnaya, V. Zorin, Evaluation of temoporfin affinity to β-cyclodextrins assuming self-aggregation, J. Photochem. Photobiol. Chem. 367 (2018) 13–21. doi:10.1016/j.jphotochem.2018.07.046.
[116] V.J. Stella, Q. He, Cyclodextrins, Toxicol. Pathol. 36 (2008) 30–42. doi:10.1177/0192623307310945.
[117] N. Sharma, A. Baldi, Exploring versatile applications of cyclodextrins: an overview, Drug Deliv. 23 (2016) 729–747. doi:10.3109/10717544.2014.938839.

[118] V.J. Stella, V.M. Rao, E.A. Zannou, V. Zia, Mechanisms of drug release from cyclodextrin complexes, Adv. Drug Deliv. Rev. 36 (1999) 3–16. doi:10.1016/S0169-409X(98)00052-0.
[119] L. Li, K.M. Huh, Polymeric nanocarrier systems for photodynamic therapy, Biomater. Res. 18 (2014) 19. doi:10.1186/2055-7124-18-19.
[120] C.F. van Nostrum, Polymeric micelles to deliver photosensitizers for photodynamic therapy, Adv. Drug Deliv. Rev. 56 (2004) 9–16. doi:10.1016/j.addr.2003.07.013.
[121] Y. Nakamura, A. Mochida, P.L. Choyke, H. Kobayashi, Nanodrug Delivery: Is the Enhanced Permeability and Retention Effect Sufficient for Curing Cancer?, Bioconjug. Chem. 27 (2016) 2225–2238. doi:10.1021/acs.bioconjchem.6b00437.
[122] V.P. Torchilin, Structure and design of polymeric surfactant-based drug delivery systems, J. Control. Release Off. J. Control. Release Soc. 73 (2001) 137–172.
[123] M. Anaya, M. Kwak, A.J. Musser, K. Müllen, A. Herrmann, Tunable Hydrophobicity in DNA Micelles: Design, Synthesis, and Characterization of a New Family of DNA Amphiphiles, Chem. – Eur. J. 16 (2010) 12852–12859. doi:10.1002/chem.201001816.
[124] J. Li, H. Pei, B. Zhu, L. Liang, M. Wei, Y. He, N. Chen, D. Li, Q. Huang, C. Fan, Self-assembled multivalent DNA nanostructures for noninvasive intracellular delivery of immunostimulatory CpG oligonucleotides, ACS Nano. 5 (2011) 8783–8789. doi:10.1021/nn202774x.
[125] I. Brezaniova, J. Trousil, Z. Cernochova, V. Kral, M. Hruby, P. Stepanek, M. Slouf, Self-assembled chitosan-alginate polyplex nanoparticles containing temoporfin, Colloid Polym. Sci. 295 (2017) 1259–1270. doi:10.1007/s00396-016-3992-6.
[126] J.-M. Lü, X. Wang, C. Marin-Muller, H. Wang, P.H. Lin, Q. Yao, C. Chen, Current advances in research and clinical applications of PLGA-based nanotechnology, Expert Rev. Mol. Diagn. 9 (2009) 325–341. doi:10.1586/erm.09.15.
[127] J. Sun, W. Birnbaum, J. Anderski, M.-T. Picker, D. Mulac, K. Langer, D. Kuckling, Use of light-degradable aliphatic polycarbonate nanoparticles as drug carrier for photosensitizer, Biomacromolecules. (2018). doi:10.1021/acs.biomac.8b01446.
[128] T.A. Debele, S. Peng, H.-C. Tsai, Drug Carrier for Photodynamic Cancer Therapy, Int. J. Mol. Sci. 16 (2015) 22094–22136. doi:10.3390/ijms160922094.
[129] Yan Fei, Kopelman Raoul, The Embedding of Meta-tetra(Hydroxyphenyl)-Chlorin into Silica Nanoparticle Platforms for Photodynamic Therapy and Their Singlet Oxygen Production and pH-dependent Optical Properties¶, Photochem. Photobiol. 78 (2007) 587–591. doi:10.1562/0031-8655(2003)0780587TEOMIS2.0.CO2.
[130] D. Liu, B. Lin, W. Shao, Z. Zhu, T. Ji, C. Yang, In Vitro and in Vivo Studies on the Transport of PEGylated Silica Nanoparticles across the Blood–Brain Barrier, ACS Appl. Mater. Interfaces. 6 (2014) 2131–2136. doi:10.1021/am405219u.
[131] S. Hanada, K. Fujioka, Y. Inoue, F. Kanaya, Y. Manome, K. Yamamoto, Cell-Based in Vitro Blood–Brain Barrier Model Can Rapidly Evaluate Nanoparticles' Brain Permeability in Association with Particle Size and Surface Modification, Int. J. Mol. Sci. 15 (2014) 1812–1825. doi:10.3390/ijms15021812.
[132] J. Kreuter, Influence of the surface properties on nanoparticle-mediated transport of drugs to the brain, J. Nanosci. Nanotechnol. 4 (2004) 484–488.
[133] D. Verma, N. Gulati, S. Kaul, S. Mukherjee, U. Nagaich, Protein Based Nanostructures for Drug Delivery, J. Pharm. (2018). doi:10.1155/2018/9285854.
[134] E. Reddi, Role of delivery vehicles for photosensitizers in the photodynamic therapy of tumours, J. Photochem. Photobiol. B. 37 (1997) 189–195. doi:10.1016/S1011-1344(96)07404-0.

[135] M. Wacker, K. Chen, A. Preuss, K. Possemeyer, B. Roeder, K. Langer, Photosensitizer loaded HSA nanoparticles. I: Preparation and photophysical properties, Int. J. Pharm. 393 (2010) 254–263. doi:10.1016/j.ijpharm.2010.04.022.
[136] A. Puri, K. Loomis, B. Smith, J.-H. Lee, A. Yavlovich, E. Heldman, R. Blumenthal, Lipid-Based Nanoparticles as Pharmaceutical Drug Carriers: From Concepts to Clinic, Crit. Rev. Ther. Drug Carrier Syst. 26 (2009) 523–580.
[137] V.P. Torchilin, Recent advances with liposomes as pharmaceutical carriers, Nat. Rev. Drug Discov. 4 (2005) 145–160. doi:10.1038/nrd1632.
[138] M.D. Vetta, L. González, J.J. Nogueira, Hydrogen Bonding Regulates the Rigidity of Liposome-Encapsulated Chlorin Photosensitizers, ChemistryOpen. 7 (2018) 475–483. doi:10.1002/open.201800050.
[139] J. Kuntsche, I. Freisleben, F. Steiniger, A. Fahr, Temoporfin-loaded liposomes: Physicochemical characterization, Eur. J. Pharm. Sci. 40 (2010) 305–315. doi:10.1016/j.ejps.2010.04.005.
[140] N. Düzgüneş, S. Nir, Mechanisms and kinetics of liposome–cell interactions, Adv. Drug Deliv. Rev. 40 (1999) 3–18. doi:10.1016/S0169-409X(99)00037-X.
[141] V. Reshetov, D. Kachatkou, T. Shmigol, V. Zorin, M.-A. D'Hallewin, F. Guillemin, L. Bezdetnaya, Redistribution of meta-tetra(hydroxyphenyl)chlorin (m-THPC) from conventional and PEGylated liposomes to biological substrates, Photochem. Photobiol. Sci. 10 (2011) 911–919. doi:10.1039/C0PP00303D.
[142] H. Hefesha, S. Loew, X. Liu, S. May, A. Fahr, Transfer mechanism of temoporfin between liposomal membranes, J. Controlled Release. 150 (2011) 279–286. doi:10.1016/j.jconrel.2010.09.021.
[143] S. Holzschuh, K. Kaeß, G.V. Bossa, C. Decker, A. Fahr, S. May, Investigations of the influence of liposome composition on vesicle stability and drug transfer in human plasma: a transfer study, J. Liposome Res. 28 (2018) 22–34. doi:10.1080/08982104.2016.1247101.
[144] D. Kachatkou, S. Sasnouski, V. Zorin, T. Zorina, M.-A. D'Hallewin, F. Guillemin, L. Bezdetnaya, Unusual photoinduced response of mTHPC liposomal formulation (Foslip), Photochem. Photobiol. 85 (2009) 719–724. doi:10.1111/j.1751-1097.2008.00466.x.
[145] M.H. Teiten, L. Bezdetnaya, J.L. Merlin, C. Bour-Dill, M.E. Pauly, M. Dicato, F. Guillemin, Effect of meta-tetra(hydroxyphenyl)chlorin (mTHPC)-mediated photodynamic therapy on sensitive and multidrug-resistant human breast cancer cells, J. Photochem. Photobiol. B. 62 (2001) 146–152.
[146] V. Reshetov, H.-P. Lassalle, A. François, D. Dumas, S. Hupont, S. Gräfe, V. Filipe, W. Jiskoot, F. Guillemin, V. Zorin, L. Bezdetnaya, Photodynamic therapy with conventional and PEGylated liposomal formulations of mTHPC (temoporfin): comparison of treatment efficacy and distribution characteristics in vivo, Int. J. Nanomedicine. 8 (2013) 3817–3831. doi:10.2147/IJN.S51002.
[147] R. van der Meel, M.H.A.M. Fens, P. Vader, W.W. van Solinge, O. Eniola-Adefeso, R.M. Schiffelers, Extracellular vesicles as drug delivery systems: lessons from the liposome field, J. Control. Release Off. J. Control. Release Soc. 195 (2014) 72–85. doi:10.1016/j.jconrel.2014.07.049.
[148] G. Fuhrmann, A. Serio, M. Mazo, R. Nair, M.M. Stevens, Active loading into extracellular vesicles significantly improves the cellular uptake and photodynamic effect of porphyrins, J. Controlled Release. 205 (2015) 35–44. doi:10.1016/j.jconrel.2014.11.029.
[149] R.H. Müller, K. Mäder, S. Gohla, Solid lipid nanoparticles (SLN) for controlled drug delivery – a review of the state of the art, Eur. J. Pharm. Biopharm. 50 (2000) 161–177. doi:10.1016/S0939-6411(00)00087-4.

[150] V.J. Lingayat, N.S. Zarekar, R.S. Shendge, Solid Lipid Nanoparticles: A Review, Nanosci. Nanotechnol. Res. 4 (2017) 67–72. doi:10.12691/nnr-4-2-5.
[151] F.P. Navarro, G. Creusat, C. Frochot, A. Moussaron, M. Verhille, R. Vanderesse, J.-S. Thomann, P. Boisseau, I. Texier, A.-C. Couffin, M. Barberi-Heyob, Preparation and characterization of mTHPC-loaded solid lipid nanoparticles for photodynamic therapy, J. Photochem. Photobiol. B. 130 (2014) 161–169. doi:10.1016/j.jphotobiol.2013.11.007.
[152] S. Haupt, I. Lazar, H. Weitman, M.O. Senge, B. Ehrenberg, Pdots, a new type of nanoparticle, bind to mTHPC via their lipid modified surface and exhibit very high FRET efficiency between the core and the sensitizer, Phys Chem Chem Phys. 17 (2015) 11412–11422. doi:10.1039/C4CP05579A.
[153] T. Murakami, H. Nakatsuji, M. Inada, Y. Matoba, T. Umeyama, M. Tsujimoto, S. Isoda, M. Hashida, H. Imahori, Photodynamic and Photothermal Effects of Semiconducting and Metallic-Enriched Single-Walled Carbon Nanotubes, J. Am. Chem. Soc. 134 (2012) 17862–17865. doi:10.1021/ja3079972.
[154] B. McCormack, G. Gregoriadis, Entrapment of cyclodextrin-drug complexes into liposomes: potential advantages in drug delivery, J. Drug Target. 2 (1994) 449–454. doi:10.3109/10611869408996821.
[155] S. Franzè, U.M. Musazzi, P. Minghetti, F. Cilurzo, Drug-in-micelles-in-liposomes (DiMiL) systems as a novel approach to prevent drug leakage from deformable liposomes, Eur. J. Pharm. Sci. Off. J. Eur. Fed. Pharm. Sci. 130 (2019) 27–35. doi:10.1016/j.ejps.2019.01.013.
[156] J. Chen, W.-L. Lu, W. Gu, S.-S. Lu, Z.-P. Chen, B.-C. Cai, X.-X. Yang, Drug-in-cyclodextrin-in-liposomes: a promising delivery system for hydrophobic drugs, Expert Opin. Drug Deliv. 11 (2014) 565–577. doi:10.1517/17425247.2014.884557.
[157] P. Mura, F. Maestrelli, M. Cecchi, M. Bragagni, A. Almeida, Development of a new delivery system consisting in ‘drug–in cyclodextrin–in PLGA nanoparticles,’ J. Microencapsul. 27 (2010) 479–486. doi:10.3109/02652040903515508.
[158] S. Rawal, M.M. Patel, Threatening cancer with nanoparticle aided combination oncotherapy, J. Controlled Release. 301 (2019) 76–109. doi:10.1016/j.jconrel.2019.03.015.